ORGANOMETALLICS

pubs.acs.org/Organometallics Article

Silver(I) N-Heterocyclic Carbene Complexes Derived from Clotrimazole: Antiproliferative Activity and Interaction with an Artificial Membrane-Based Biosensor

Heba A. Mohamed, Samantha Shepherd, Nicola William, Helen A. Blundell, Madhurima Das, Christopher M. Pask, Benjamin R. M. Lake, Roger M. Phillips,* Andrew Nelson,* and Charlotte E. Willans*

Cite This: https://dx.doi.org/10.1021/acs.organomet.0c00069 Read Online

ACCESS | Metrics & More | Article Recommendations | Supporting Information

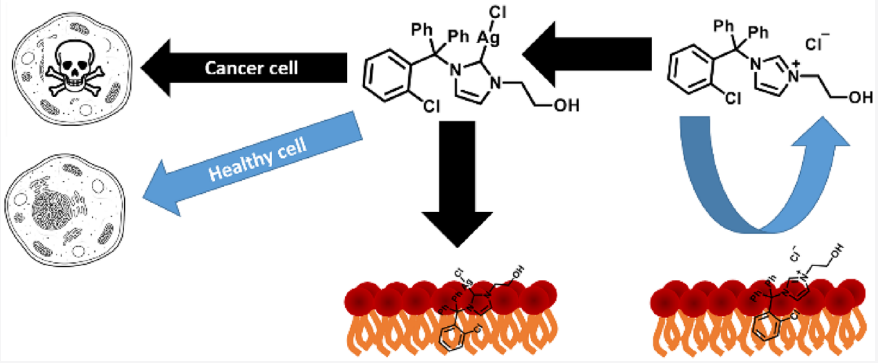

ABSTRACT: With the aim of combining the potential anticancer properties of both clotrimazole, an imidazole based antifungal agent, and silver(I) N-heterocyclic carbenes, 13 novel silver(I) N-heterocyclic carbene complexes derived from clotrimazole were synthesized. The complexes were fully characterized, and the partition coefficient of each was determined to provide a measure of hydrophobicity. The antiproliferative properties of the complexes against cancerous and noncancerous cell lines found optimum cytotoxicity when the complex displays an "intermediate lipophilicity", which describes a complex that possesses both water-soluble groups and lipophilic aromatic groups. The silver complexes were screened on a synthetic biomembrane-like device using a chip-based phospholipid-coated Pt/Hg electrode embedded in a flow cell system. The results are recorded as rapid cyclic voltammograms (RCVs), which give insight into the interactions of the complexes with a cell membrane. Interestingly the principle of "intermediate lipophilicity" also applies to the monolayer interaction to which the silver atom significantly implements an irreversibility.

INTRODUCTION

The serendipitous discovery of cisplatin as an anticancer agent by Rosenberg at the end of the 1960s opened up a new area of research in organometallic chemistry for the treatment of cancer.[1] Despite the success of cisplatin and other platinum-based drugs, severe side effects and the development of drug resistance are drawbacks to their clinical applications.[2,3] Therefore, research efforts have also examined the potential of other metals as chemotherapeutic agents. Complexes of ruthenium,[4−6] iron,[7] and titanium[8] exhibit significant cytotoxic effects, with some ruthenium complexes having undergone clinical trials.[9] Silver is another metal that has been studied for its biomedicinal properties, as it is thought to have relatively low toxicity, and the antimicrobial properties of this metal have been exploited for centuries.[10] In recent years, studies have shown that silver also has potential in the field of cancer chemotherapy.[11−13]

Over the last few decades, N-heterocyclic carbenes (NHCs) have become ubiquitous ligands in organometallic chemistry, particularly in the field of catalysis.[14−23] In recent years, metal-NHCs have shown promise in biomedical applications, including as antimicrobial (silver-NHCs) and as antitumor (palladium-, copper-, silver-, gold-, ruthenium-, and platinum-NHCs) agents.[12,24−41] The efficacy of a silver-based drug appears to be linked to its bioavailability,[29,42] which is affected by, for example, its solubility and the presence of biological ligands and halides. The release rate of silver from a prodrug is

Received: February 3, 2020

linked to the ancillary ligand, and as NHCs are strong σ donors, silver-NHCs can have a slow silver release rate. It is imperative that the ligand also have a low toxicity profile.

Clotrimazole (Figure 1A) is an imidazole-containing compound and is a highly effective treatment for fungal diseases in plants, humans, and animals.[43] It is a readily available material that is already present in many pharmaceutical treatments, administered both orally and topically for infections such as dermatophytes and staphylococci. Once administered, clotrimazole can be metabolized and excreted from the body (Figure 1B,C).[44] Clotrimazole also shows activity against various tumor cell lines and is thought to be effective by decreasing the movement of intracellular Ca^{2+} and K^{+} ions.[45] Its ability to interact with cell membranes and penetrate cells can be attributed to its aromaticity.[46] As clotrimazole is an imidazole-containing compound, possessing negligible toxicity and anticancer properties, it is an ideal precursor to silver-NHCs for examination as chemotherapeutic agents. Herein we report the synthesis, characterization, and bioactivity of a family of silver(I)-NHCs prepared from clotrimazole-derived imidazolium salts. The complexes were screened against cancerous cell lines, including the pancreatic cancer cell lines Panc 10.05 and MIA PaC-2, and the colorectal carcinoma BE cell line, plus the noncancerous cell line APRE-19 in order to assess both their cytotoxicity and selectivity. As clotrimazole inhibits proliferating cells by affecting the transport of ions across the plasma membrane,[45] the silver complexes and corresponding ligand precursors have been screened on a biosensing device which measures their interaction with a phospholipid sensor element, to provide an indication of their biological membrane activity.[47]

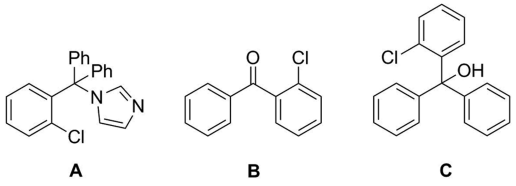

Figure 1. Active antifungal compound clotrimazole (A) and its metabolites 2-chlorobenzophenone (B) and (2-chlorophenyl)-diphenylmethanol (C).

RESULTS AND DISCUSSION

Imidazolium salts **1a,c** were prepared using microwave conditions (Scheme 1A) and fully characterized. Crystals suitable for X-ray crystallography were grown via diffusion of diethyl ether into a solution of either **1a** or **1c** in dichloromethane (see the Supporting Information). The solid-state structures show the expected imidazolium iodide salts, with no evidence of hydrogen-bonding or anion$-\pi$ interactions between the iodide anion and the imidazolium ring.[48] Such interactions are likely to be precluded by the presence of the bulky trityl group adjacent to the imidazolium ring. Interestingly, an anion$-\pi$ interaction does appear to exist between the aryl chloride and the imidazolium ring in **1c**, with an aryl-Cl$\cdots$imidazolium centroid distance of 3.28 Å. In contrast to **1a,c**, we found that imidazolium salt **1e** could instead be prepared more efficiently through the reaction of the reagents in dichloromethane at reflux (Scheme 1B). Crystals suitable for X-ray crystallography were grown via diffusion of diethyl ether into a solution of **1e** in dichloromethane. The structure shows the expected imidazolium salt;

Scheme 1. Synthesis of Imidazolium Salts 1a,c,e starting from Clotrimazole (A, B), 2a−e Starting from 2-Chlorotrityl Chloride (C), and 3a−e Starting from Trityl Chloride (D) and Silver-NHC Complexes[a]

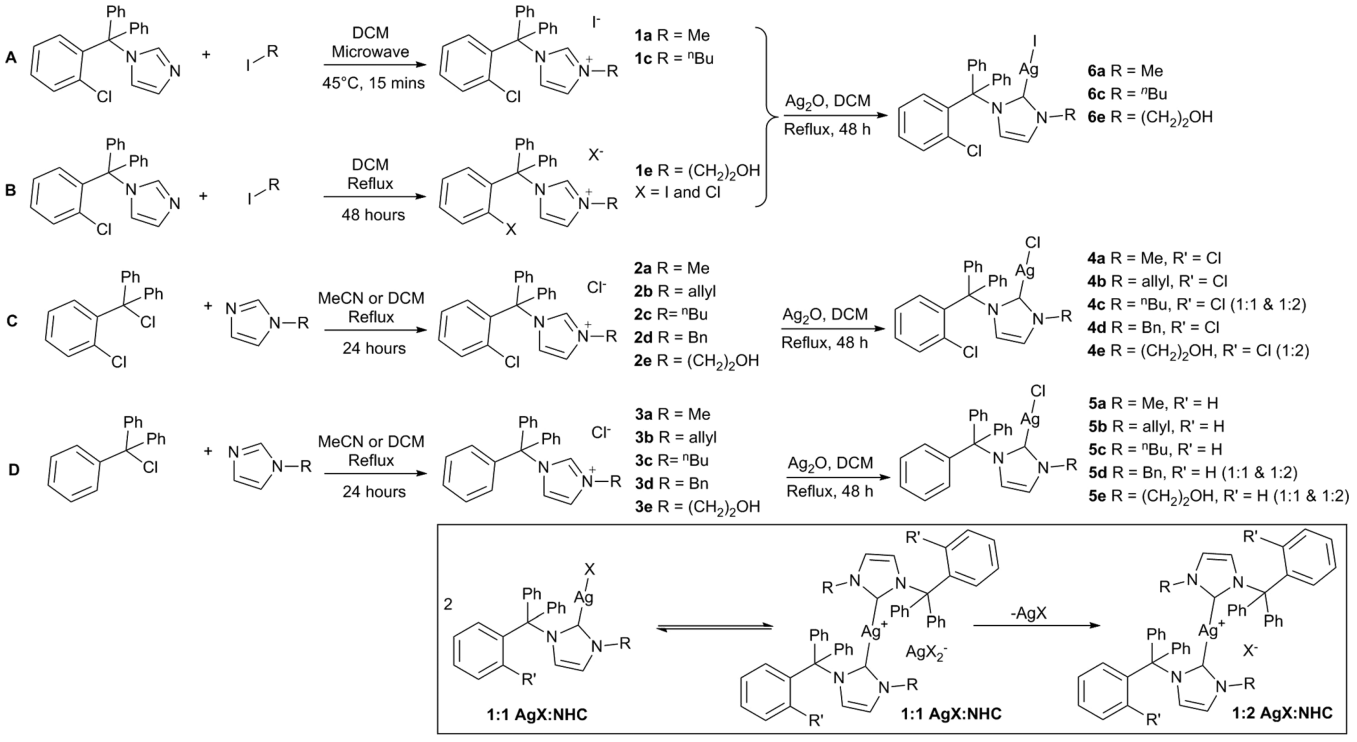

[a]In the box are shown solution equilibria between 2Ag(NHC)X and $[Ag(NHC)_2]AgX_2$ with removal of AgX to form $[Ag(NHC)_2]X$.

https://dx.doi.org/10.1021/acs.organomet.0c00069
Organometallics XXXX, XXX, XXX−XXX

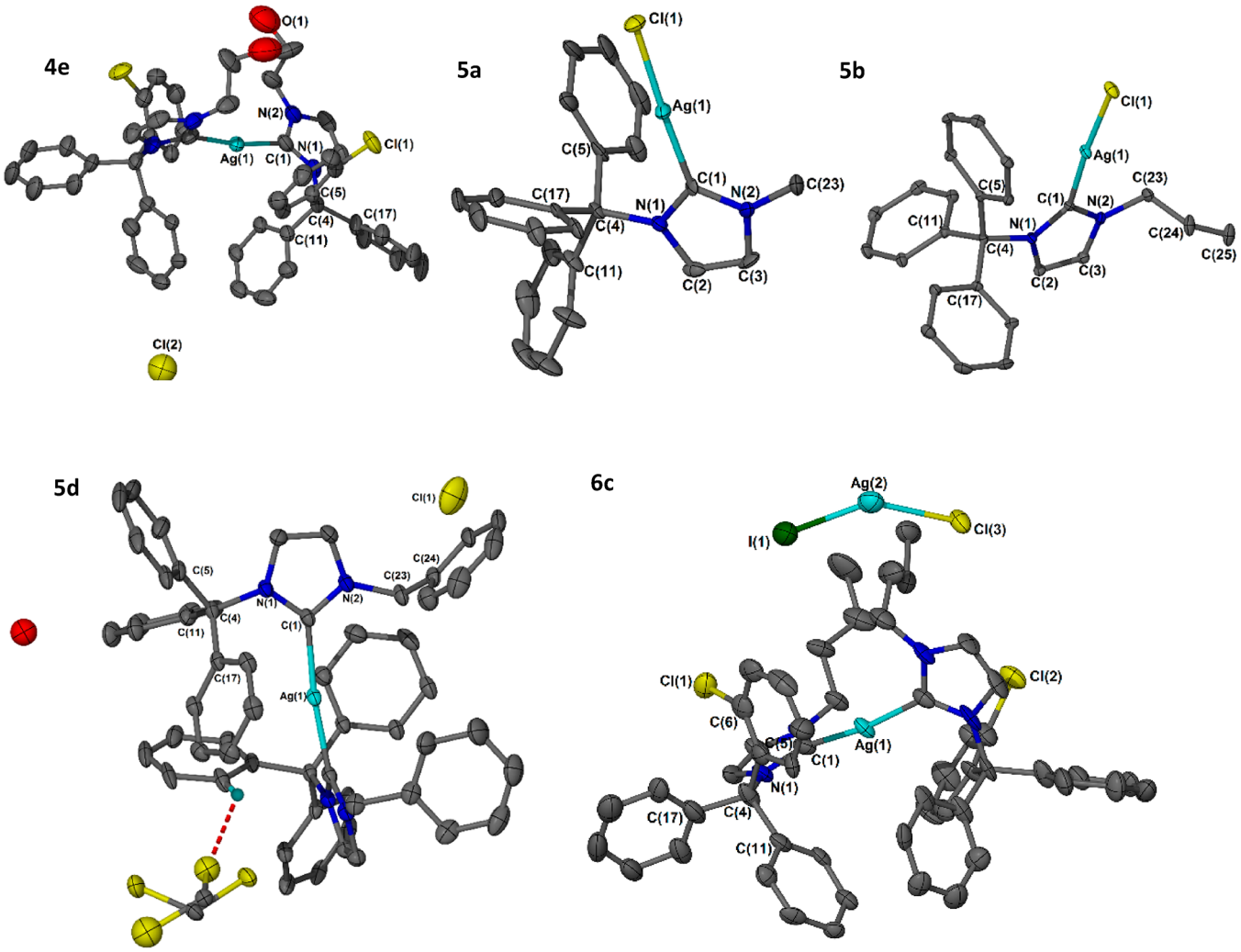

Figure 2. Molecular structures of silver-NHC complexes **4e**, **5a**,**b**,**d**, and **6c**. Hydrogen atoms and water molecules have been omitted for clarity. Ellipsoids are shown at 50% probability for **5a**,**b**, 40% for **5d**, and 35% for **4e** and **6c**.

however, the anion (labeled I(1)) is substitutionally disordered, containing a mixture of chloride (29%) and iodide (71%) (see the Supporting Information). The chloride may originate from impurities in the dichloromethane solvent; however, it is likely that this observation is a result of exchange between the iodide anion and the chloride of the 2-chlorotrityl group. This is further evidenced through the aryl halide group (labeled Cl(1)) also being present as a mixture of chloride (97%) and iodide (3%). To prevent the formation of imidazolium salts with disordered halides, N-substituted imidazoles were reacted with 2-chlorotrityl chloride in acetonitrile or dichloromethane at reflux, to yield imidazolium compounds **2a**−**e** (Scheme 1C). With the intent of investigating the effect of the 2-chlorotrityl group within the ligand on the anticancer activity of the silver complexes, a second set of imidazolium compounds **3a**−**e** were synthesized in the same manner, starting with trityl chloride (Scheme 1D). The compounds were fully characterized, with crystals of **2a**,**b**,**d**,**e** and **3e** suitable for X-ray diffraction analysis being grown by diffusion of either diethyl ether or pentane into either a dichloromethane or methanol solution of the compounds (see the Supporting Information).

Reaction of the imidazolium salts with Ag_2O resulted in the formation of complexes of the type Ag(NHC)X (where X = halide), $[Ag(NHC)_2]X$ (where X = halide and/or AgX_2^-), or a combination of the two. Solution equilibria between 2Ag(NHC)X and $[Ag(NHC)_2]AgX_2$ is a common phenomenon observed in silver-NHCs and is not observed on the NMR time scale here (Scheme 1).[13,29,49−51] Equilibration of these species is known to occur on very different time scales in different media.[52] As the complexes were filtered through Celite during workup, some AgX was removed from the bis-NHCs, resulting in X rather than AgX_2 counterions in the cationic species (X = Cl, I). Silver-NHC complexes were fully characterized using NMR spectroscopy, high-resolution mass spectrometry, and elemental analysis, which revealed the ratios of X^- to AgX_2^- counteranions, and solid-state structures were obtained for complexes **4e**, **5a**,**b**,**d**, and **6c** (Figure 2). The molecular structures reveal that the mono- and bis-NHC complexes have similar bond distances between the silver and the carbenic carbon atoms (2.08−2.12 Å) and similar NCN bond angles between the carbenic carbon and neighboring nitrogen atoms (103−106°). The geometry around the silver centers distort slightly from linearity, with $C_{carbene}$−Ag−$C_{carbene}$/X bond angles ranging 171.2(7)° for **6c** to 176.42(14) ° for **5a**.

As a means to assess the affinity of complexes **4**−**6** for the phospholipid component of the cell membrane, the partition

https://dx.doi.org/10.1021/acs.organomet.0c00069
Organometallics XXXX, XXX, XXX−XXX

coefficient (log *P*) of the 13 complexes and cisplatin was measured. The results are summarized in Figure 3, with log *P*

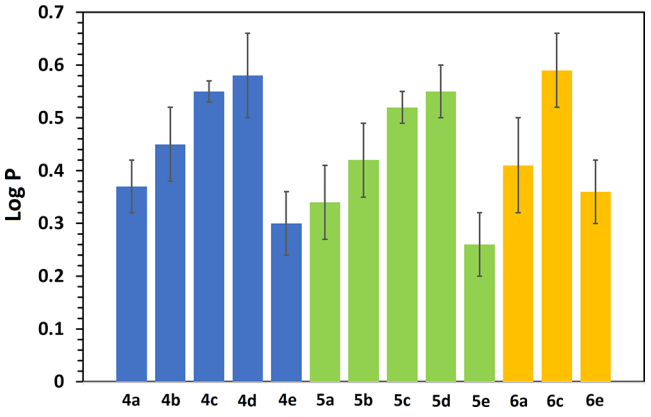

Figure 3. Bar chart to show the log *P* values for complexes **4**–**6**.

values ranging from 0.26(±0.06) (**5e**) to more hydrophobic 0.59(±0.07) (**6c**). Cisplatin, with a log *P* value of −1.35(±0.26), is more hydrophilic than any of the silver-NHC complexes tested. Three trends relating to hydrophobicity can be observed from Figure 3. (i) Complexes **4a**–**e**, with a Cl substituent on the triphenyl group, appear to be more hydrophobic than the corresponding complexes **5a**–**e**, where the Cl is replaced with a H. (ii) The benzyl-containing complexes **4d** and **5d** are the most hydrophobic in their series followed by butyl-, allyl-, methyl-, and hydroxyethyl-containing complexes. (iii) Substituting the chloride counterion for an iodide anion in complexes **6a**,**c**,**e** increases the hydrophobicity of the complexes in comparison to their analogous chloride complexes **4a**,**c**,**e**. The higher lipophilicity of complexes **6a**,**c**,**e** was anticipated, as a larger iodide anion with a higher molar mass provides greater polarizability than a chloride anion. The *in vitro* cytotoxicity of silver-NHC complexes **4**–**6** was determined using MTT-based assays following a 96 h drug-exposure period. Compounds were initially tested for their activity against pancreatic adenocarcinoma cell line Panc 10.05 and the noncancerous ARPE-19 cell line. Compounds with a selectivity index (defined as the ratio of mean IC_{50} values for ARPE-19 cells divided by the mean IC_{50} in cancer cells) higher than that of cisplatin (**4a**,**e** and **5e**) were evaluated further by assessing their antiproliferative activity against pancreatic carcinoma MIA PaC-2 and colorectal carcinoma BE. Complexes **4b**,**d** and **6a**,**c**,**e** were also tested against all four cell lines to determine whether low selectivity ratios were also observed in other cell lines, and the results are summarized in Figure 4 and Table 1. From the MTT assays it can be seen that the 2-chlorotrityl-bearing silver-NHC complexes **4a**–**e** are generally more cytotoxic against Panc 10.05 than their corresponding trityl-bearing complexes **5a**–**e**, indicating that the presence of an aryl-Cl group plays a role in the activity of these complexes. This could be due to the fact that the Cl group increases the propensity of the complexes to interact with phospholipid and cell membranes.[53] Complex **4e** is the most active against Panc 10.05 of all 13 complexes tested and exhibits an IC_{50} value which is comparable to that of cisplatin ($p > 0.05$). The hydroxyethyl group increases the hydrophilicity of the complex (lower log *P*), thus enhancing the water solubility, which also improves the cytotoxicity. Changing the counterion from chloride on complex **4c** to iodide in complex **6c** improves the cytotoxicity against Panc 10.05 ($p < 0.01$). However, when iodide complex **6e** was tested against Panc 10.05, it revealed a numerically inferior activity in comparison to its corresponding chloride-containing analogue **4e** (although the difference did not reach statistical significance; $p > 0.05$), with complexes **4a** (chloride) and **6a** (iodide) exhibiting activities similar to each other ($p > 0.05$). In general, iodide-containing complexes such as **6c** displays comparable cytotoxicity against all cell lines tested in comparison to its chloride analogues **4a** ($p > 0.05$) and **4c** ($p > 0.05$) when the N substituent is methyl or *n*butyl. The reverse is observed when the N substituent is hydroxyethyl, with chloride-containing complex **4e** displaying greater cytotoxicity in comparison to its iodide analogue **6e** against Panc 10.0 cells ($p < 0.05$). This difference was cell line dependent, however, with **6e** showing greater activity against BE cells in comparison to **4e** (although this did not reach statistical significance; $p > 0.05$). These differences in trend indicate that there is a fine balance between groups within the overall complex, with modification of one moiety influencing the effect of another.

All of the silver complexes were evaluated against the noncancerous retinal epithelial cell line ARPE-19 to evaluate

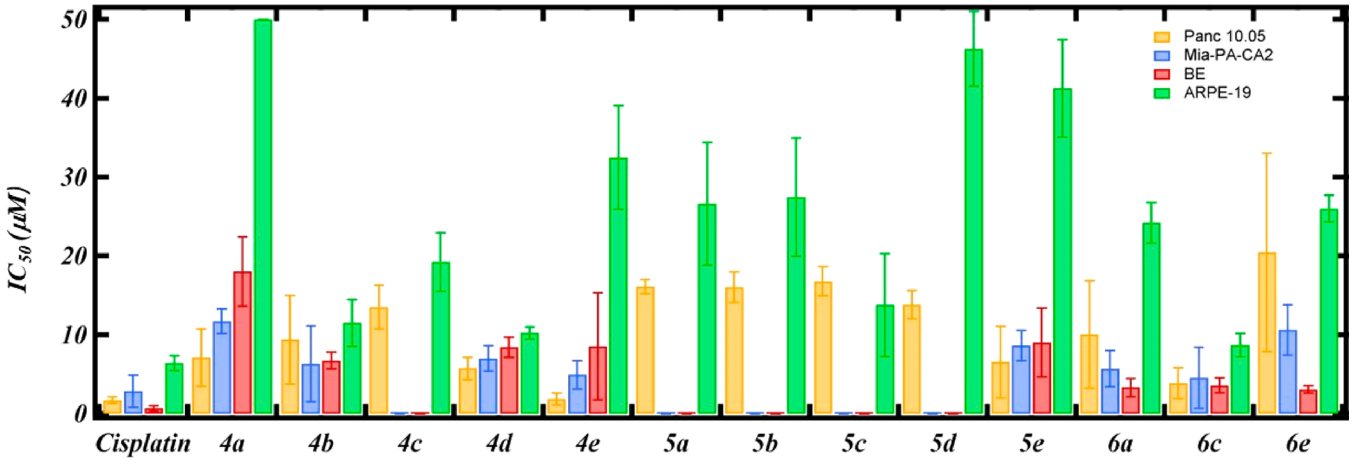

Figure 4. Bar chart to show IC_{50} values for complexes **4**–**6** in comparison to those of cisplatin against Panc 10.05, MIA PaCa-2, and BE cancerous cell lines and the ARPE-19 noncancerous cell line.

https://dx.doi.org/10.1021/acs.organomet.0c00069
Organometallics XXXX, XXX, XXX−XXX

Table 1. Responses of Panc 10.05, Mia-PaCa-2, and BE Cancerous Cell Lines and the ARPE-19 Noncancerous Cell Line to Silver-NHC Complexes 4−6[a]

	cell line			
	Panc 10.05	Mia-PaCa-2	BE	ARPE-19
cisplatin	1.7 ± 0.4 (3.75)	2.8 ± 2.0 (2.26)	0.7 ± 0.3 (9.71)	6.4 ± 0.9
4a	7.1 ± 3.7 (7.04[b])	11.7 ± 1.6 (4.27[b])	18.0 ± 4.4 (2.77[b])	>50
4b	9.4 ± 5.6 (1.22)	6.3 ± 4.8 (1.82)	6.7 ± 1.1 (1.71)	11.5 ± 2.9
4c	13.5 ± 2.8 (1.42)			19.2 ± 3.7
4d	5.8 ± 1.4 (1.78)	7.0 ± 1.6 (1.46)	8.4 ± 1.2 (1.21)	10.2 ± 0.8
4e	1.9 ± 0.7 (17.47)	4.9 ± 1.8(6.62)	8.5 ± 6.8 (3.80)	32.5 ± 6.6
5a	16.1 ± 0.9 (1.66)			26.6 ± 7.8
5b	16.1 ± 1.9 (1.71)			27.5 ± 7.5
5c	16.8 ± 1.8 (0.82)			13.8 ± 6.5
5d	13.8 ± 1.8 (3.35)			46.3 ± 4.7
5e	6.5 ± 4.5 (6.30)	8.6 ± 1.9 (4.78)	9.0 ± 4.3 (4.56)	41.2 ± 6.2
6a	10.0 ± 6.8 (2.41)	5.7 ± 2.3 (4.23)	3.3 ± 1.2 (7.31)	24.2 ± 2.6
6c	3.8 ± 1.9 (2.25)	4.5 ± 3.9 (1.91)	3.6 ± 0.9 (2.42)	8.7 ± 1.5
6e	20.5 ± 12.6 (1.27)	10.6 ± 3.2 (2.28)	3.1 ± 0.5 (8.51)	26.0 ± 1.7

[a]Values presented are IC_{50} (μM) ± SD for three independent experiments. The values in parentheses represent the selectivity ratio defined as the IC_{50} value for ARPE-19 cells divided by the IC_{50} value for each of the cancer cell lines tested. [b]Minimum possible value as the value for ARPE-19 is 50 μM (highest concentration tested).

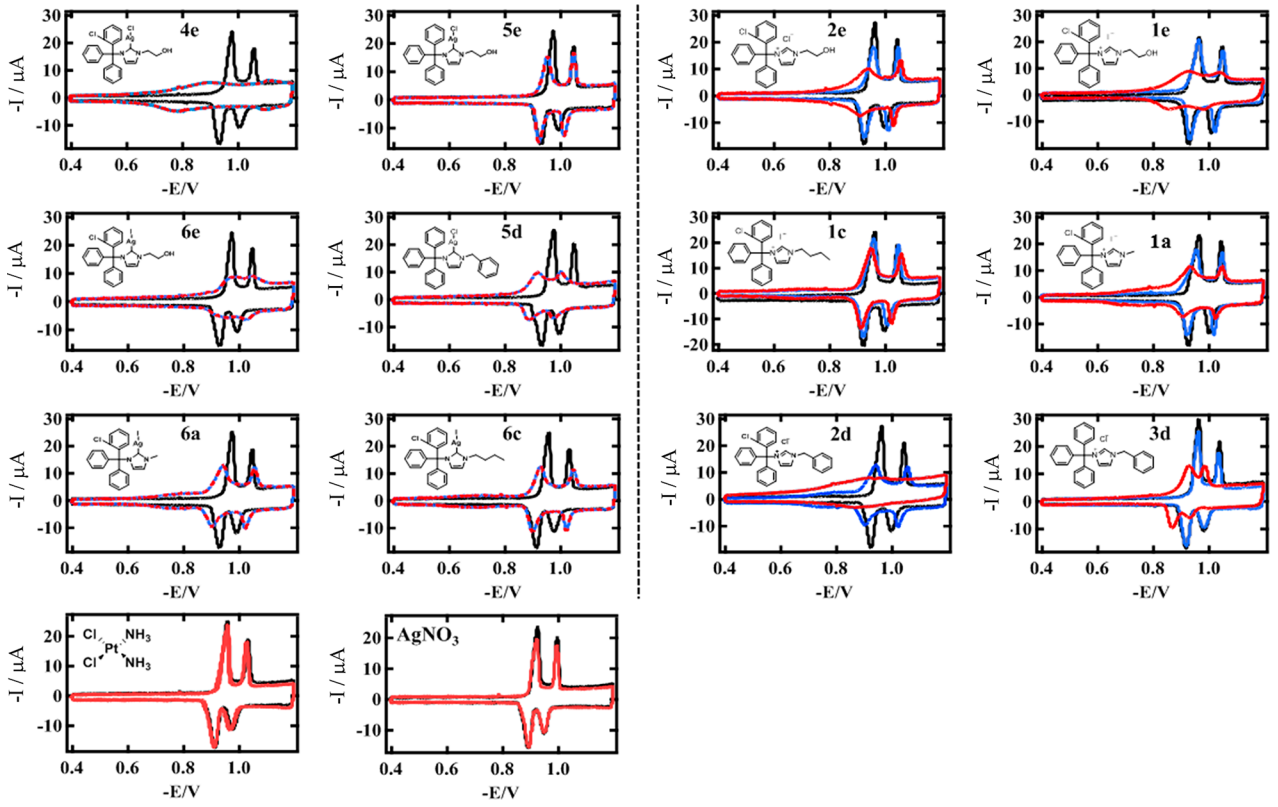

Figure 5. RCVs recorded at 40 V s^{-1} of a DOPC-coated Pt/Hg electrode (black) in the presence of 50 μM silver(I)-NHC complex (left) or clotrimazole-derived imidazolium salt (right) (red), recovery of DOPC (blue) in PBS at pH 7.4, and RCVs in the presence of 2 mM of cisplatin or $AgNO_3$ (red) in PBS at pH 7.4 (bottom).

their selectivity toward cancerous cells (Table 1). Complexes **4a,e** and **5e** show the greatest selectivity toward the cancerous Panc 10.05 over the noncancerous ARPE-19, with selectivity ratios higher than that of cisplatin. Complex **4e**, the most active of the 13 complexes, is also the most selective toward Panc 10.05, exhibiting a selectivity ratio of 17.47, which is almost 5-fold the selectivity of cisplatin. Complex **4e** also exhibits the highest selectivity ratio for cancerous MIA PaCa-2 over noncancerous ARPE-19, while **6e** displays the highest selectivity for cancerous BE over ARPE-19. Across the panel of cell lines, selectivity indices were comparable for compounds **4b,d** and **6c** (Table 1). For compounds **4e** and **6a,e**, however, selectivity ratios were cell line dependent, reflecting inherent differences in cancer cell sensitivity to these compounds (Table 1). While the SI values for **6a** (7.31) and **6e** (8.51) against BE cells were less than the SI for cisplatin (9.71), these

https://dx.doi.org/10.1021/acs.organomet.0c00069
Organometallics XXXX, XXX, XXX−XXX

results suggest that caution should be exercised with regard to selecting compounds on the basis of SI values obtained for one cell line.

Clotrimazole has been evaluated against MCF7 and MDA-MB-231 breast cancer cell lines and its activity compared with the response of nontumorigenic MCF10A cells.[54] While clotrimazole completely and preferentially inhibited the proliferation of MCF10A cells, there was selective cell kill (as determined by trypan blue exclusion, LDH release, and the MTT assay) in MCF7 and MDA-MB-231 cells. As the cells were immediately analyzed following drug exposure (24 h duration), the results are not directly comparable to the results of this study but do indicate that clotrimazole itself has some inherent selectivity for cancer cells *in vitro*.

To help assess the potential effect of silver complexes on the biomembrane, a membrane-based sensing device was utilized to test the putative biomembrane activity of the 13 complexes **4**−**6** and cisplatin.[47,55−60] This device consists of an electrode-supported monolayer of dioleoylphosphatidylcholine (DOPC), which has been validated against DOPC bilayer vesicles showing identical interactions with biomembrane-active compounds. The DOPC monolayer is deposited on a microfabricated Pt/Hg electrode that is connected to an online high-throughput flow system and utilizes rapid cyclic voltammetry (RCV) to display changes in capacitance current peaks when a voltage scan of 40 V s^{-1} is applied.[56] The DOPC monolayer undergoes two potential-induced phase transitions represented by two characteristic sharp capacitance current peaks from −0.4 to −1.2 V (vs Ag/AgCl). The two sequential reversible transitions correspond to the entrance of electrolyte into the layer coincident with pore formation and the reorganization of the layer to form a patchy bilayer, respectively.[58] The interaction of the complexes with the layer can be observed by changes in the current peak configurations representative of phospholipid monolayer damage as well as increases in the baseline capacitance current informing on how well the complexes and/or water penetrate monolayer sensor element.[60]

Initially, screening of silver complexes **4e**, **5d,e**, and **6a,c,d** prepared at 50 μM solutions displayed differences in interactions with DOPC (Figure 5, left), which could be related to variations in ligand N substituents and the presence/absence of Cl on the triphenyl group. A comparison of interactions of the hydroxyethyl-containing complexes **4e**, **5e**, and **6e** with DOPC indicates that the chloride on the triphenyl group increases the interaction with the DOPC sensor element, as **5e** shows less interaction than the chloride-containing **4e** and **6e**. The effect of chloride as an aromatic substituent in promoting interaction with the lipid has been shown previously.[53,61] Changing the N substituent from a hydroxyethyl in **6e** to a methyl in **6a** or an *n*-butyl in **6c** decreases the interaction with the sensor element, which indicates that improving the water solubility through addition of a hydroxyethyl substituent may improve the kinetics of interaction at the monolayer surface. Conversely, changing the N substituent to a benzyl appears to increase the interaction with the DOPC, even more than for hydroxyethyl, which is shown by the difference between the interactions shown by the RCVs of **5d,e**. This is not unusual, as aromatic rings are reported to promote phospholipid monolayer interactions.[53,61] The decreased interaction of **6e** in comparison to **4e** with the DOPC layer can be attributed to the larger iodide atom on **6e**, which, although it increases the hydrophobicity of the complex, has some steric or related effect which inhibits compound penetration of the DOPC monolayer. A full understanding of the extent of the interaction, however, can only be obtained by analyzing the LOD values, which also depend on the slope of the calibration curves (see the Experimental Section). The interaction of the silver complexes with DOPC is irreversible, as the RCVs of the DOPC do not return to the original state after electrolyte flushing. In general, the silver complex−DOPC interaction appears to have little to do with their rather low log *P* values and is more associated with their structure, where the clotrimazole group clearly promotes lipid monolayer interactions through its aromaticity.

Model membrane experiments have been carried out previously with an extensive series of compounds, including tricyclic antidepressant pharmaceuticals,[47] aromatic hydrocarbons,[62] flavonoids,[63] ionic liquids,[64] nanomaterials,[65] and biomembrane-active[59] and -inactive[66] peptides. Significantly this study is the first one carried out on the interaction of organometallic compounds with the phospholipid sensor element, although metal ion interactions with the element have already been investigated.[67] The clear conclusion from previous studies is that the electrochemical model membrane platform is responsive to any species which is biomembrane-active. Biomembrane activity indicates any interaction that alters the structure and organization of a biomembrane and can be, but not always is, related to lipophilicity.[62] Generally the interaction is due to an association with the phospholipid polar groups and/or phospholipid hydrocarbon tails of the phospholipid bilayer. RCVs of the imidazolium ligand precursors tested demonstrate interactions with DOPC similar to those observed for the silver complexes (Figure 5, right), with the identical structure-based interaction of variations in N substituents and the presence/absence of chloride on the triphenyl group. A comparison of interactions of ligand precursors with their corresponding silver complexes generally shows a slight decrease in the interactions of the imidazolium salts from the interactions with the silver complexes. However, most interestingly, the interaction of the clotrimazole ligand precursors, unlike that of the derived silver-NHC complexes, tends to be reversible, where the RCVs of the DOPC return in most cases almost to the original state. In the PBS electrolyte, Cl^- is the common ion where the ligand counterion is Cl^-. In the case where the ligand counterion is I^-, it is unlikely that the electrolyte Cl^- replaces the very much more polarizable I^-, where there will be an element of ion pairing with the aromatic ligand cation. The evidence shows that the nature of the counterion appears to affect the interaction and reversibility of the ligand cation's interaction with the model membrane, as shown by compounds **1e** and **2e**, respectively (Figure 5). This difference in interaction would not be observed if the counterion I^- was replaced by Cl^-. Interestingly, neither cisplatin nor $AgNO_3$ interacts with DOPC (Figure 5, bottom). This supports the knowledge of the contribution of a copper influx transporter in mediating the accumulation of cisplatin in the cell.[68] The fact that $AgNO_3$ does not interact with the lipid sensor element indicates that the silver-NHC interaction is a function of its organically bound environment. We note that this study was focused on the synthesis, cytotoxicity, and putative anticancer activity of clotrimazole silver complexes. The ligand precursor biomembrane activity was investigated together with that of the silver complexes to obtain a better understanding of what role the substituted Ag atom played in the complex bioactivity.

https://dx.doi.org/10.1021/acs.organomet.0c00069
Organometallics XXXX, XXX, XXX−XXX

The interaction of these complexes with the DOPC-coated Hg follows the received wisdom in that the chloride on the triphenyl group promotes an interaction. The rather surprising observations are that the polar hydroxyethyl N substituent also promotes an interaction and that the inserted Ag atom causes an interaction with the lipid layer to become irreversible. Such irreversibility has been seen before from interactions of a DOPC sensor element with hydrophobic substituted benzene compounds and with the more polar amine narcotics.[62] The observation of the effect of the interactions on the capacitance current−potential curves is interesting. Both the ligand precursors and silver-NHC complexes induce a depression of the capacitance current peaks and a positive potential peak shift on initial interaction. This is likely due to the positively charged ligand precursors and the partially positive Ag atom being located within the lipid polar group region.[62] With no increase in the capacitance current baseline, no penetration of the apolar region is indicated. Where a stronger interaction is noted (**4e** and **2d**), a significant increase in the capacitance current baseline is more indicative of a complete disruption of the monolayer organization which, in the case of the ligand precursor (**2d**), the interaction is partially reversible. Also noted is the interaction of compounds containing iodides (**6a**,**c** and **1a**,**c**) with the DOPC sensor element causing a slight but significant hump in the capacitance current baseline (see the Supporting Information), which presumably is the effect of the iodide moiety penetrating the monolayer.

From the LOD values of the complexes on the DOPC sensor element (Table 2), **4e** has the lowest value of 0.001 μM and **5d** has the highest value of 0.3 μM. Interestingly, **4e** also exhibits a low IC_{50} value of 1.9 ± 0.74 μM, showing a cytotoxicity against Panc 10.05 superior to those of the other complexes tested and comparable to the IC_{50} value of cisplatin (1.7 ± 0.41 μM). **5d**, on the other hand, has a relatively high IC_{50} value of 13.8 ± 1.77 μM. The data imply that several factors, in addition to lipid biomembrane damage, contribute to the cytotoxicity of the silver complexes.

Table 2. LODs Using a Phospholipid Sensing Device and IC_{50} Values toward the Panc 10.05 Cancerous Cell Line

compound	LOD (μM)	IC_{50} ± SD (μM)
4a	0.002	7.1 ± 3.67
4e	0.001	1.9 ± 0.74
5d	0.3	13.8 ± 1.77
5e	0.07	6.5 ± 4.55
6a	0.05	10.0 ± 6.79
6e	0.025	20.5 ± 12.58

CONCLUSIONS

Thirteen clotrimazole-based silver(I)-NHC complexes have been synthesized and fully characterized. The antiproliferative activities of the silver complexes were examined against pancreatic adenocarcinoma cell line Panc 10.05 and non-cancerous retinal epithelial cells ARPE-19 and compared to that of cisplatin. Selected complexes were also examined against pancreatic adenocarcinoma cell line MIA PaC-2 and colorectal carcinoma cell line BE. While most of the complexes were less potent than cisplatin against Panc 10.05, complex **4e** showed potency comparable to that of cisplatin in addition to showing 5-fold greater selectivity than cisplatin to Panc 10.05 over the noncancerous ARPE-19. Complexes **5e** and **4a** also showed improved selectivity toward Panc 10.05 over cisplatin. **4e** and **5e** exhibit "intermediate lipophilicity", where the complex contains both hydrophobic and hydrophilic groups, which plays a role in both cytotoxicity and selectivity. The hydrophilic part, which in these complexes is the hydroxyethyl group, increases their water solubility and improves their transfer at the biointerface, while the hydrophobic triphenyl group promotes an interaction with the lipid bilayers of membranes. While the chloride-containing groups **4** and **5** appear to be consistent in their cytotoxicity trends, iodide-containing complexes **6a**,**c**,**e** show different trends in cytotoxicity across the different cancerous cell lines, indicating that their activity is tumor type dependent. The introduction of a silver atom to the clotrimazole-derived compounds renders their interaction with an electrode-supported DOPC sensor element irreversible. The heterocyclic N-substituted hydroxyethyl chain and a chloride atom on the triphenyl group enhance the activity of the ligand precursors and the silver(I)-NHC complexes with the DOPC sensor element. The silver complex showing the strongest interaction with the biomembrane-like sensor element had an IC_{50} value very close to that of cisplatin. These results help validate this electrochemical platform as an early-stage screen, i.e. prior to cell studies, for pharma candidates where the mode of action is structure related and lipid membrane based.

EXPERIMENTAL SECTION

General Methods. Where stated, manipulations were performed under an atmosphere of dry nitrogen by means of standard Schlenk line techniques. Anhydrous solvents were prepared by passing the solvent over activated alumina to remove water, copper catalyst to remove oxygen, and molecular sieves to remove any remaining water, via the Dow−Grubbs solvent system. ^{1}H and $^{13}C\{^{1}H\}$ NMR spectra were recorded on either a Bruker DPX300 or a Bruker AV500 spectrometer. The values of chemical shifts are given in ppm and values for coupling constants (J) in Hz. Mass spectra were collected on a Bruker Daltonics (micro TOF) instrument operating in the electrospray mode. Microanalyses were performed using a Carlo Erba MOD 1106 Elemental Analyzer. X-ray diffraction data were collected on either a Bruker Nonius X8 diffractometer fitted with an Apex II detector with Mo Kα radiation (λ = 0.71073 Å) or an Agilent SuperNova diffractometer fitted with an Atlas CCD detector with Mo Kα radiation (λ = 0.71073 Å) or Cu Kα radiation (λ = 1.5418 Å). Crystals were mounted under oil on glass or nylon fibers. Data sets were corrected for absorption using a multiscan method, and the structures were solved by direct methods using SHELXS-97 and refined by full-matrix least squares on F^2 using ShelXL-97.[69,70] Molecular graphics for all structures were generated using POV-RAY in the X-Seed program.

Synthesis of Imidazolium Iodide 1a. Clotrimazole (0.20 g, 0.58 mmol) and methyl iodide (0.72 mL, 11.60 mmol) were dissolved in dichloromethane (3 mL) and heated to 45 °C in the microwave for 15 min with stirring. Diethyl ether was added to the resulting pale yellow solution, which induced precipitation of the product as an off-white solid. This was filtered, washed with diethyl ether, and dried *in vacuo*. Yield: 0.21 g (75%). ^{1}H NMR ($CDCl_3$, 300 MHz): δ 9.10 (s, 1H, NCHN), 7.75 (s, 1H, NCH), 7.50−7.11 (m, 14H, aromatic), 6.95 (s, 1H, NCH), 4.25 (s, 3H, CH_3). $^{13}C\{^{1}H\}$ NMR ($CDCl_3$, 75 MHz): δ 138.0 (CH), 137.9 (C), 137.4 (C), 135.1 (C), 132.9 (CH), 131.7 (CH), 131.5 (CH), 130.1 (CH), 192.5 (CH), 129.2 (CH), 128.1 (CH), 124.1 (CH), 123.6 (CH), 79.5 (C), 38.8 (CH_3). HRMS (ESI+): calcd for $C_{23}H_{20}ClN_2$ $[M - I]^+$, 359.1310; found 359.1311. Anal. Calcd for $C_{23}H_{26}ClIN_2 \cdot 1/3H_2O$: C, 56.06; H, 4.23; N, 5.68. Found: C, 56.00; H, 4.10; N, 5.70. Single crystals suitable for X-ray diffraction analysis were grown by the vapor diffusion of diethyl ether into a concentrated solution of the product in dichloromethane.

https://dx.doi.org/10.1021/acs.organomet.0c00069
Organometallics XXXX, XXX, XXX−XXX

Synthesis of Imidazolium Iodide 1c. Clotrimazole (0.20 g, 0.58 mmol) and butyl iodide (0.67 mL, 5.80 mmol) were dissolved in dichloromethane (3 mL) and heated to 45 °C in the microwave for 15 min with stirring. Diethyl ether was added to the resulting pale yellow solution, which induced precipitation of the product as a white solid. This was filtered, washed with diethyl ether, and dried *in vacuo*. Yield: 0.18 g (59%). ^{1}H NMR ($CDCl_3$, 300 MHz): δ 9.18 (s, 1H, NCHN), 7.71(s, 1H, NCH), 7.51−6.91 (m, 14H, aromatic), 6.74 (s, 1H, NCH), 4.63 (t, J = 7.3 Hz, 2H, CH_2), 1.86 (m, 2H, CH_2), 1.37 (m, 2H, CH_2), 0.93 (t, J = 7.3 Hz, 3H, CH_3). ^{13}C{^{1}H} NMR ($CDCl_3$, 75 MHz): δ 140.3 (C), 138.1 (C), 137.1 (CH), 135.5 (C), 132.1 (CH), 131.4 (CH), 130.0 (CH), 129.7 (CH), 129.0 (CH), 127.9 (CH), 127.0 (CH), 123.6 (CH), 121.5 (CH), 79.1 (C), 50.9 (CH_2), 32.3 (CH_2), 19.2 (CH_2), 13.5 (CH_3). HRMS (ESI+): calcd for $C_{26}H_{26}ClN_2$ [M − I]$^+$, 401.1785; found, 401.1778. Anal. Calcd for $C_{26}H_{24}ClIN_2 \cdot 1/2H_2O$: C, 58.06; H, 5.06; N, 5.21. Found: C, 58.30; H, 4.90; N, 5.30. Single crystals suitable for X-ray diffraction analysis were grown by the vapor diffusion of diethyl ether into a concentrated solution of the product in dichloromethane.

Synthesis of Imidazolium Iodide 1e. Clotrimazole (0.50 g, 1.45 mmol) and iodoethanol (0.23 mL, 2.9 mmol) were dissolved in dichloromethane (3 mL) and heated at reflux under nitrogen for 48 h, resulting in a brown solution. Addition of ethyl acetate precipitated a yellow soli,d which was filtered and washed with ethyl acetate. Trituration with acetone gave the product as a white solid. Yield: 0.38 g (47%). ^{1}H NMR ($CDCl_3$, 300 MHz): δ 9.04 (s, 1H, NCHN), 7.75 (s, 1H, NCH), 7.52−7.10 (m, 14H, aromatic), 7.02 (s, 1H, NCH), 4.64 (t, J = 4.9 Hz, 2H, CH_2), 3.99 (t, J = 4.9 Hz, 2H, CH_2), 2.82 (broad s, 1H, OH). ^{13}C{^{1}H} NMR ($CDCl_3$, 75 MHz): δ 138.1 (C), 137.8 (CH), 137.4 (C), 135.3 (C), 133.0 (CH), 131.5 (CH), 131.4 (CH), 130.0 (CH), 129.5 (CH), 129.2 (CH), 128.1 (CH), 123.5 (CH), 123.4 (CH) 79.3 (C), 59.9 (CH_2), 52.8 (CH_2). HRMS (ESI +): calcd for $C_{24}H_{22}ClN_2O$ [M − I]$^+$, 389.1421; found, 389.1419. Anal. Calcd for $C_{24}H_{22}ClIN_2O$: C, 55.78; H, 4.29; N, 5.42. Found: C, 56.00; H, 4.40; N, 5.90. Single crystals suitable for X-ray diffraction analysis were grown by the vapor diffusion of diethyl ether into a concentrated solution of the product in methanol.

Synthesis of Imidazolium Chloride 2a. 2-Chlorotrityl chloride (0.50 g, 1.60 mmol) and 1-methylimidazole (0.50 mL, 6.27 mmol) were dissolved in acetonitrile (10 mL) and heated at reflux for 24 h. The solution was cooled to room temperature, and the product was precipitated as a white solid using diethyl ether. Yield: 0.53 g (85%). ^{1}H NMR ($CDCl_3$, 300 MHz): δ 9.10 (s, 1H, NCHN), 7.75 (s, 1H, NCH), 7.50−7.11 (m, 14H, aromatic), 6.95 (s, 1H, NCH), 4.25 (s, 3H, CH_3). ^{13}C{^{1}H} NMR ($CDCl_3$, 75 MHz): δ 139.1 (CH), 138.4 (C), 137.6 (C), 135.4 (C), 133.0(CH), 131.7 (CH), 131.4 (CH), 130.0 (CH), 129.5 (CH), 129.1 (CH), 127.9 (CH), 123.7 (CH), 123.4 (CH), 79.3 (C), 37.8 (CH_3). HRMS (ESI+): calcd for $C_{23}H_{20}ClN_2$ [M − Cl]$^+$, 359.1310; found, 359.1311. Single crystals suitable for X-ray diffraction analysis were grown by the vapor diffusion of pentane into a concentrated solution of the product in dichloromethane.

Synthesis of Imidazolium Chloride 2b. 2-Chlorotrityl chloride (0.50 g, 1.60 mmol) and 1-allylimidazole (0.48 mL, 4.40 mmol) were dissolved in acetonitrile (10 mL) and heated at reflux for 24 h. The yellow solution was cooled to room temperature, and a yellow oil formed on addition of diethyl ether. The solution was decanted from the oil, which was washed with ethyl acetate and triturated with acetone to give the product as a white solid that was dried *in vacuo*. Yield: 0.37 g (55%). ^{1}H NMR ($CDCl_3$, 300 MHz): δ 9.84 (s, 1H, NCHN), 7.71 (s, 1H, NCH), 7.51−7.06 (m, 14H, aromatic), 6.96 (s, 1H, NCH), 6.08−5.95 (m, 1H, CH), 5.41−5.35 (m, 4H, NCH_2CHCH_2). ^{13}C{^{1}H} NMR ($CDCl_3$, 75 MHz): δ 138.8 (CH), 138.4 (C), 137.5 (C), 135.4 (C), 132.9 (CH), 131.8 (CH), 131.5 (CH), 130.8 (CH), 130.0 (CH), 129.5 (CH),129.1 (CH), 127.9 (CH), 123.5 (CH), 122.2 (CH), 121.9 (CH_2) 79.4 (C), 52.9 (CH_2). HRMS (ESI+): calcd for $C_{25}H_{22}ClN_2$ [M − Cl]$^+$, 385.1466; found, 385.1471. Single crystals suitable for X-ray diffraction analysis were grown by the vapor diffusion of diethyl ether into a concentrated solution of the product in dichloromethane.

Synthesis of Imidazolium Chloride 2c. 2-Chlorotrityl chloride (0.50 g, 1.60 mmol) was dissolved in dichloromethane (5 mL), and 1-butylimidazole (0.21 mL, 1.60 mmol) was added. The mixture was transferred to an ampule and heated at 45 °C for 24 h in a closed system. Excess diethyl ether was added to the resulting yellow solution to obtain a white solid. Yield: 0.30 g (43%). ^{1}H NMR ($CDCl_3$, 300 MHz): δ 9.60 (s, 1H, NCHN), 8.19 (s, 1H, NCH), 7.47−6.98 (m, 15H, aromatic and NCH), 4.63 (t, 2H, CH_2), 1.84 (pent, 2H, CH_2), 1.28 (sext, 2H, CH_2), 0.86 (t, 3H, CH_3). ^{13}C{^{1}H} NMR ($CDCl_3$, 75 MHz): δ 138.5 (C), 138.2 (CH), 137.5 (C), 135.3 (C), 132.9 (CH), 131.8 (CH), 131.4 (CH), 129.8 (CH), 129.3 (CH), 129.0 (CH), 127.9 (CH), 123.6 (CH), 122.7 (CH), 79.1 (C), 50.5 (CH_2), 32.5 (CH_2), 19.4 (CH_2), 13.6 (CH_3). HRMS (ESI+): calcd for $C_{26}H_{26}ClN_2$ [M − Cl]$^+$, 401.1779; found, 401.1764. Anal. Calcd for $C_{26}H_{26}Cl_2N_2$: C, 71.39; H, 5.99; N, 6.90. Found: C, 71.10; H, 6.20; N, 6.60.

Synthesis of Imidazolium Chloride 2d. 2-Chlorotrityl chloride (0.50 g, 1.60 mmol) and 1-benzylimidazole (0.25 mL, 1.93 mmol) were dissolved in acetonitrile (10 mL) and heated at reflux for 24 h. The solution was cooled to room temperature, and a yellow solid was precipitated using diethyl ether. This was filtered and washed with ethyl acetate and acetone to give a white solid, which was dried *in vacuo*. Yield: 0.14 g (20%). ^{1}H NMR ($CDCl_3$, 300 MHz): δ 9.92 (s, 1H, NCHN), 7.49 (s, 1H, NCH), 7.44−7.02 (m, 19H, aromatic), 6.88 (s, 1H, NCH), 5.90 (s, 2H, CH_2). ^{13}C{^{1}H} NMR ($CDCl_3$, 75 MHz): δ 157.7 (C), 138.9 (CH), 138.5 (C), 137.5 (C), 135.4 (C), 133.7 (CH), 132.9 (CH), 131.9 (CH), 131.4 (CH), 129.9 (CH),129.4 (CH), 129.3 (CH), 129.1 (CH), 129.1 (CH), 127.9 (CH), 123.5 (CH), 122.1 (C), 79.3 (CH_2), 54.1 (CH_2). HRMS (ESI +): calcd for $C_{29}H_{24}ClN_2$ [M − Cl]$^+$, 435.1623; found, 435.1630. Single crystals suitable for X-ray diffraction analysis were grown by the vapor diffusion of diethyl ether into a concentrated solution of the product in dichloromethane.

Synthesis of Imidazolium Chloride 2e. 2-Chlorotrityl chloride (1.0 g, 3.20 mmol) was dissolved in dichloromethane (5 mL) in an ampule, to which 1-(2-hydroxyethyl)imidazole (0.30 mL, 3.20 mmol) was added. The solution was heated to 45 °C for 24 h in a closed system. Excess pentane was added to the yellow solution, yielding a yellow oil, which was further recrystallized from methanol/pentane to obtain a yellow solid. Yield: 1.32 g (97%). ^{1}H NMR (d_6-acetone, 300 MHz): δ 8.98 (s, 1H, NCHN), 7.68 (s, 1H, NCH), 6.91 (s, 1H, NCH), 7.87−7.12 (m, 14H, aromatic), 4.41 (t, J = 12 Hz, 2H, CH_2), 3.87 (t, J = 12 Hz, 2H, CH_2). ^{1}H NMR (d_4-MeOD, 300 MHz): δ 9.00 (s, 1H, NCHN), 7.83 (s, 1H, NCH), 7.64−7.20 (m, 15H, aromatic and NCH), 4.41 (t, 2H, CH_2), 3.89 (t, 2H, CH_2). ^{13}C{^{1}H} NMR (d_6-acetone, 125 MHz): δ 139.0 (C), 138.2 (CH), 135.4 (C), 133.2 (C), 132.1 (CH), 131.8 (CH), 130.4 (CH), 129.8 (CH), 129.3 (CH), 128.5 (CH), 127.8 (CH), 124.6 (CH), 123.8 (CH), 120.6 (C), 79.2 (C), 61.6 (CH_2), 60.2 (CH_2). HRMS (ESI+): calcd for $C_{24}H_{22}ClN_2O$ [M − Cl]$^+$, 389.1421; found, 389.1425. Anal. Calcd for $C_{24}H_{22}Cl_2N_2O \cdot 1/4H_2O$: C, 67.06; H, 5.28; N, 6.52. Found: C, 67.20; H, 5.25; N, 6.70. Single crystals suitable for X-ray diffraction analysis were grown by the vapor diffusion of diethyl ether into a concentrated solution of the product in methanol.

Synthesis of Imidazolium Chloride 3a. Trityl chloride (6.80 g, 24.40 mmol) and 1-methylimidazole (2 g, 24.40 mmol) were dissolved in acetonitrile (20 mL) and heated at reflux for 24 h. The solution was cooled, and a white solid was obtained with the addition of excess diethyl ether. Yield: 6.1 g, (69%). ^{1}H NMR (300 MHz, $CDCl_3$): δ 9.50 (s, 1H, NCHN), 7.90 (s, 1H, NCH), 7.42−7.12 (m, 15H, aromatic), 6.97 (s, 1H, NCH), 4.29 (s, 3H, CH_3). ^{13}C{^{1}H} NMR (125 MHz, $CDCl_3$): δ 147.0 (CH), 139.6 (CH), 138.0 (CH), 135.9 (CH), 129.7 (CH), 129.3 (CH), 129.0 (CH), 128.0 (CH), 127.9 (CH), 127.2 (CH), 124.1 (CH), 123.8 (CH), (CH), 122.1 (CH), 119.9 (CH), 79.5 (C), 36.2 (CH_3). HRMS (ESI+): calcd for $C_{23}H_{21}N_2$ [M − Cl]$^+$, 325.1699; found, 325.1701. Anal. Calcd for $C_{23}H_{21}ClN_2.2H_2O$: C, 69.60; H, 6.35; N, 7.06. Found: C, 69.80; H, 6.30; N, 7.40.

Synthesis of Imidazolium Chloride 3b. Trityl chloride (5.15 g, 18.50 mmol) and 1-allyl-1*H*-imidazole (0.58 g, 1.49 mmol) were

https://dx.doi.org/10.1021/acs.organomet.0c00069
Organometallics XXXX, XXX, XXX−XXX

dissolved in dichloromethane (20 mL) and heated at reflux for 24 h. Addition of excess diethyl ether gave a white solid that was dried *in vacuo*. Yield: 3.03 g, (42%). ^{1}H NMR (300 MHz, $CDCl_3$): δ 9.62 (s, 1H, NCHN), 7.81 (s, 1H, NCH), 7.41−7.11 (m, 15H, aromatic), 6.98 (s, 1H, NCH), 6.10−5.97 (m, 1H, CH), 5.43−5.35 (m, 4H, N−CH_2CHCH_2). ^{13}C{^{1}H} NMR (125 MHz, $CDCl_3$): δ 139.6 (CH), 138.5 (C), 138.0 (CH), 130.6 (CH), 130.3 (CH), 129.6 (CH), 129.6 (CH), 129.1 (CH), 128.9 (CH), 128.6 (CH), 127.9 (CH), 127.6 (CH), 126.6 (CH), 126.4 (CH), 125.7 (CH), 123.8 (CH), 122.2 (CH_2), 52.8 (CH_2). HRMS (ESI+): calcd for $C_{25}H_{23}N_2$ [M − Cl]$^+$, 351.1856; found, 351.4187. Anal. Calcd for $C_{25}H_{23}ClN_2$: C, 72.02; H, 6.37; N, 6.72. Found: C, 71.80; H, 6.30; N, 6.90.

Synthesis of Imidazolium Chloride 3c. Trityl chloride (1.35 g, 4.84 mmol) and 1-butylimidazole (0.60 g, 4.84 mmol) were dissolved in dichloromethane (20 mL) and heated at reflux for 24 h. Excess diethyl ether was added to the solution to obtain an off white solid. A saturated solution of $NaHCO_3$ (20 mL) was added to the solid and the product was extracted into dichloromethane (3 × 20 mL). Recrystallization from dichloromethane/diethyl ether yielded a white solid which was dried *in vacuo*. Yield: 0.99 g (51%). ^{1}H NMR (300 MHz, $CDCl_3$): δ 9.46 (s, 1H, NCHN), 7.99 (s, 1H, NCH), 7.43−7.03 (m, 15H, aromatic), 7.01 (s, 1H, NCH), 4.69 (t, 2H, CH_2), 1.85 (q, 2H, CH_2), 1.31 (sext, 2H, CH_2), 0.97 (t, 3H, CH_3). ^{13}C{^{1}H} NMR (75 MHz, $CDCl_3$): δ 139.6 (CH), 138.1 (C), 137.6 (CH), 136.3 (CH), 135.3 (CH), 133.5 (CH), 131.3 (CH), 130.4 (CH), 129.6 (CH), 129.3 (CH), 128.9 (CH), 127.7 (CH), 126.3 (CH), 125.7 (CH), 124.3 (Ar), 123.9, (CH), 50.5 (CH_2), 32.3 (CH_2), 19.5 (CH_2), 13.5 (CH_3). HRMS (ESI+): calcd for $C_{26}H_{27}N_2$ [M − Cl]$^+$, 367.2169; found, 367.2119. Anal. Calcd for $C_{26}H_{27}ClN_2{\cdot}4/3H_2O$: C, 73.14; H, 7.00; N, 6.56. Found: C, 73.10; H, 6.90; N, 6.80.

Synthesis of Imidazolium Chloride 3d. Trityl chloride (0.50 g, 1.79 mmol) and 1-benzylimidazole (0.28 g, 1.79 mmol) were dissolved in dichloromethane (5 mL). The solution was transferred to an ampule and heated at 45 °C for 24 h in a closed system. Excess diethyl ether was added to the solution to acquire an off-white solid, which was filtered and dried *in vacuo*. A saturated solution of $NaHCO_3$ (20 mL) was added to the solid, and the product was extracted into dichloromethane (3 × 20 mL). Excess diethyl ether was added to the solution, furnishing a white solid, which was dried *in vacuo*. Yield: 0.51 g (71%). ^{1}H NMR (500 MHz, $CDCl_3$): δ 9.82 (s, 1H, NCHN), 7.71 (s, 1H, NCH), 6.93 (s, 1H, NCH), 7.46−7.11 (m, 20H, aromatic), 5.94 (s, 2H, CH_2). ^{13}C{^{1}H} NMR (75 MHz, $CDCl_3$): δ 138.2 (CH), 135.5 (C), 129.6 (CH), 129.5 (CH), 129.4 (CH), 129.3 (CH), 129.2 (CH), 128.9 (CH), 127.9 (CH), 127.2 (CH), 123.7 (CH), 122.0 (CH), 121.0 (CH), 52.93 (CH_2). HRMS (ESI+): calcd for $C_{29}H_{25}N_2$ [M − Cl]$^+$, 401.2012; found, 401.2016. Anal. Calcd for $C_{29}H_{25}ClN_2{\cdot}H_2O$: C, 76.55; H, 5.98; N, 6.16. Found: C, 76.10; H, 5.90; N, 6.60.

Synthesis of Imidazolium Chloride 3e. Trityl chloride (0.50 g, 1.80 mmol) was dissolved in dichloromethane (5 mL) in an ampule, to which 1-(2-hydroxyethyl)imidazole (0.17 mL, 1.80 mmol) was added. The solution was heated to 45 °C for 72 h in a closed system. A white solid precipitated out of the solution, which was filtered off and recrystallized from methanol/pentane, giving a white solid that was further dried *in vacuo*. Yield: 0.66 g (94%). ^{1}H NMR (300 MHz, d_4-MeOD): δ 8.89 (s, 1H, NCHN), 8.24 (s, 1H, NCH), 7.79 (s, 1H, NCH), 7.50−7.24 (m, 15H, aromatic), 4.37 (t, 2H, J = 10.5 Hz, CH_2), 4.24 (t, 2H, J = 10.5 Hz, CH_2). ^{13}C{^{1}H} NMR (300 MHz, d_4-MeOD): δ 141.4 (C), 139.4 (C), 130.8 (CH), 130.3 (CH), 129.9 (CH), 125.5 (CH), 123.9 (CH), 60.9 (CH_2), 53.5 (CH_2). HRMS (ESI+): calcd for $C_{24}H_{23}N_2O$ [M − Cl]$^+$, 355.1810; found, 355.1813. Anal. Calcd for $C_{24}H_{23}ClN_2O{\cdot}4/3H_2O$: C, 69.47; H, 6.23; N, 9.00. Found: C, 69.00; H, 6.00; N, 9.26. Single crystals suitable for X-ray diffraction analysis were grown by the vapor diffusion of diethyl ether into a concentrated solution of the product in methanol.

Synthesis of Silver Complex 4a. Imidazolium salt **2a** (0.50 g, 1.27 mmol) and silver oxide (0.29 g, 1.27 mmol) were dissolved in dichloromethane (10 mL) and heated at reflux for 24 h in the dark. The mixture was cooled and filtered over Celite, with the solid being washed with dichloromethane. The solvent was removed from the filtrate and the solid dried *in vacuo* to give the product as a white crystalline solid. Yield: 0.39 g (62%). ^{1}H NMR (300 MHz, $CDCl_3$): δ 7.44−7.42 (m, 2H, NCH and aromatic), 7.36−7.09 (m, 14H, aromatic), 6.95 (m, 1H, NCH), 3.88 (s, 3H, CH_3). ^{13}C{^{1}H} NMR (75 MHz, $CDCl_3$): δ 140.9 (C), 140.0 (C), 135.7 (C), 132.5 (CH), 131.5 (CH), 130.6 (CH), 130.5 (CH), 128.4 (CH), 128.1 (CH), 127.8 (CH), 123.6 (CH), 119.7 (CH), 77.7 (C), 40.2 (CH_3). HRMS (ESI+): calcd for $C_{46}H_{38}AgCl_2N_4$ [2M − $AgCl_2$]$^+$, 825.1521; found, 825.1520. Anal. Calcd for $C_{23}H_{19}AgCl_2N_2{\cdot}2/3CH_2Cl_2$: C, 50.87; H, 3.67; N, 5.01. Found: C, 50.90; H, 4.10; N, 4.60.

Synthesis of Silver Complex 4b. Imidazolium salt **2b** (0.30 g, 0.71 mmol) and silver oxide (0.17 g, 0.71 mmol) were dissolved in dichloromethane (8 mL) and heated at reflux for 24 h in the dark. The mixture was cooled and filtered over Celite, with the solid being washed with dichloromethane. The solvent was removed from the yellow filtrate and the solid dried *in vacuo* to give the product as a white solid. Yield: 0.14 g, (38%). ^{1}H NMR (300 MHz, $CDCl_3$): δ 7.36−7.04 (m, 15H, aromatic and NCH), 6.88 (s, 1H, NCH), 5.87 (m, 1H, NCH_2CHCH_2), 5.24−5.12 (m, 2H, N−CH_2CHCH_2), 4.71 (d, 2H, N−CH_2CHCH_2). ^{13}C{^{1}H} NMR (125 MHz, $CDCl_3$): δ 139.9 (C), 135.8 (C), 132.7 (CH), 132.6 (CH), 131.7 (CH), 130.7 (CH), 130.6 (C), 128.5 (CH), 128.2 (CH), 128.0 (CH), 123.9 (CH), 119.5 (CH), 118.5 (CH_2), 77.6 (C), 55.6 (CH_2). HRMS (ESI+): calcd for $C_{50}H_{44}AgCl_2N_4$ [2M − $AgCl_2$]$^+$, 877.1834; found, 877.1830. Anal. Calcd for $C_{25}H_{21}AgCl_2N_2{\cdot}1/2H_2O$: C, 55.89; H, 4.13; N, 5.21. Found: C, 55.50; H, 4.20; N, 5.00.

Synthesis of Silver Complex 4c. Imidazolium salt **2c** (0.02 g, 0.05 mmol) and silver oxide (0.006 g, 0.03 mmol) were dissolved in a mixture of anhydrous methanol (3 mL) and dichloromethane (3 mL) in a Schlenk flask. The mixture was stirred at room temperature for 24 h in the dark. The mixture was filtered over Celite and the solvent removed from the filtrate *in vacuo* to give the product as a light yellow solid. Yield: 0.005 g (20%). ^{1}H NMR (300 MHz, $CDCl_3$): δ 7.61−6.88 (m, 16H, aromatic and NCH), 4.15 (t, 2H, N−$CH_2CH_2CH_2CH_3$), 1.83 (m, 2H, N−$CH_2CH_2CH_2CH_3$), 1.57 (m, 2H, $NCH_2CH_2CH_2CH_3$), 0.92 (m, 3H, $NCH_2CH_2CH_2CH_3$). ^{13}C{^{1}H} NMR (75 MHz, $CDCl_3$): δ 141.2 (C), 139.6 (C), 138.4 (CH), 135.4 (C), 132.4 (CH), 131.4 (CH), 130.3 (CH), 129.7 (CH), 129.0 (CH), 128.4 (CH), 128.1 (CH), 127.8 (CH), 123.6 (CH), 118.2 (CH), 77.4 (C), 53.2 (CH_2), 33.2 (CH_2), 19.5 (CH_2), 13.7 (CH_3). HRMS (ESI+): calcd for $C_{52}H_{50}AgCl_2N_4$ [2M − $AgCl_2$]$^+$, 909.2460; found, 909.2609. Anal. Calcd for $C_{130}H_{125}Ag_4Cl_9N_{10}$, i.e. 3:1 Ag(NHC)Cl:[Ag(NHC)$_2$]Cl: C, 60.57; H, 4.89; N, 5.43. Found: C, 60.80; H, 4.80; N, 5.10.

Synthesis of Silver Complex 4d. Imidazolium salt **2d** (0.10 g, 0.21 mmol) and silver oxide (0.05 g, 0.21 mmol) were dissolved in dichloromethane (8 mL) and heated at reflux for 24 h in the dark. The mixture was filtered over Celite with the solid being washed with dichloromethane, and the solvent was removed from the filtrate. The solid was dried *in vacuo* to give the product as an off-white solid. Yield: 0.06 g (50%). ^{1}H NMR (300 MHz, $CDCl_3$): δ 7.46−7.10 (m, 20H, aromatic and NCH), 6.87 (s, 1H, NCH), 5.35 (s, 2H, CH_2). ^{13}C{^{1}H} NMR (75 MHz, $CDCl_3$): δ 141.0 (C), 139.9 (C), 135.8 (C), 135.6 (C), 132.7 (CH), 131.7 (CH), 130.7 (CH), 129.2 (CH), 128.8 (CH), 128.6 (CH),128.2 (CH), 128.1 (CH), 127.8 (CH), 127.1 (CH), 78.0 (C), 57.2 (CH_2). HRMS (ESI+): calcd for $C_{58}H_{46}AgCl_2N_4$ [2M − $AgCl_2$]$^+$, 977.2147; found, 977.2170. Anal. Calcd for $C_{29}H_{23}AgCl_2N_2{\cdot}2H_2O$: C, 56.70; H, 4.43; N, 4.56. Found: C, 56.80; H, 4.60; N, 4.10.

Synthesis of Silver Complex 4e. Imidazolium salt **2e** (0.2 g, 0.47 mmol) and silver oxide (0.065 g, 0.28 mmol) were dissolved in a solvent mixture of anhydrous methanol (10 mL) and anhydrous dichloromethane (5 mL) in a Schlenk flask with 4 Å activated molecular sieves. The mixture was stirred at room temperature for 24 h in the dark. The mixture was filtered over Celite and the solvent removed from the filtrate *in vacuo* to give the product as a white solid. Yield: 0.13 g (56%). ^{1}H NMR (300 MHz, d_4-MeOD): δ 7.52−6.99 (m, 16H, aromatic and NCH), 3.65−3.60 (m, 4H, CH_2). ^{13}C{^{1}H} NMR (75 MHz, d_4-MeOD): δ 142.3 (C), 141.6 (C), 137.2 (C), 133.8 (CH), 132.5 (CH), 131.9 (CH), 131.6 (CH), 129.6 (CH),

https://dx.doi.org/10.1021/acs.organomet.0c00069
Organometallics XXXX, XXX, XXX−XXX

129.1 (CH), 128.1 (CH), 124.9 (CH), 120.6 (CH), 78.7 (C), 62.5 (CH_2), 56.6 (CH_2). HRMS (ESI+): calcd for $C_{48}H_{42}AgCl_2N_4O_2$ [2M − $AgCl_2$]$^+$, 885.1732; found, 885.1747. Anal. Calcd for $C_{48}H_{42}AgCl_3N_4O_2$: C, 62.59; H, 4.60; N, 6.08. Found: C, 63.20; H, 5.30; N, 5.90. Single crystals suitable for X-ray diffraction analysis were grown by the vapor diffusion of diethyl ether into a concentrated solution of the product in methanol.

Synthesis of Silver Complex 5a. Imidazolium salt **3a** (0.50 g, 1.38 mmol) and silver oxide (0.32 g, 1.38 mmol) were dissolved in dichloromethane (30 mL) and heated at reflux for 18 h in the dark. The mixture was filtered over Celite and the solvent removed from the filtrate *in vacuo* to give a brown solid. Recrystallization from dichloromethane/diethyl ether gave the product as a white solid. Yield: 0.4 g (62%). ^{1}H NMR (300 MHz, $CDCl_3$): δ 7.34−7.20 (m, 15H, aromatic), 7.04 (s, 1H, NCH), 6.98 (s, 1H, NCH), 3.84 (s, 3H, CH_3). ^{13}C{^{1}H} NMR (75 MHz, $CDCl_3$): δ 140.5 (C), 129.6 (CH), 128.5 (CH), 128.2 (CH), 127.9 (CH), 122.0(HC), 119.8 (CH), 36.12 (CH_3). HRMS (ESI+): calcd for $C_{46}H_{40}AgN_4$ [2M − $AgCl_2$]$^+$, 757.2301; found, 757.2314. Anal. Calcd for $C_{23}H_{20}AgClN_2{\cdot}2/3H_2O$: C, 57.58; H, 4.48; N, 5.84. Found: C, 57.90; H, 4.60; N, 5.40. Single crystals suitable for X-ray diffraction analysis were grown by the vapor diffusion of diethyl ether into a concentrated solution of the product in dichloromethane.

Synthesis of Silver Complex 5b. Imidazolium salt **3b** (0.58 g, 1.49 mmol) and silver oxide (0.35 g, 1.49 mmol) were dissolved in dichloromethane (30 mL) and heated at reflux for 18 h in the dark. The mixture was filtered over Celite and the solvent removed from the filtrate in vacuo to give a colorless oil. Recrystallization from dichloromethane/diethyl ether gave the product as a white solid. Yield: 0.41 g (55%). ^{1}H NMR (300 MHz, $CDCl_3$): δ 7.37−7.19 (m, 15H, aromatic), 7.07 (s, 1H, NCH), 6.95 (s, 1H, NCH), 6.00 (m, 1H, N−CH_2CHCH$_2$), 5.24 (m, 2H, N−CH_2CHCH$_2$), 4.75 (d, 2H, N−CH_2CHCH$_2$). ^{13}C{^{1}H} NMR (75 MHz, $CDCl_3$): δ 142.1 (C), 132.6 (NCH), 130.6 (NCH), 129.6 (CH), 128.9 (CH), 128.6 (CH), 127.7 (CH), 119.5 (HC), 117.5 (CH_2), 55.6 (CH_2). HRMS (ESI+): calcd for $C_{50}H_{44}AgN_4$ [2M − $AgCl_2$]$^+$, 809.2614; found, 809.2616. Anal. Calcd for $C_{25}H_{22}AgClN_2$: C, 60.81; H, 4.49; N, 5.67. Found: C, 60.61; H, 4.50; N, 5.60. Single crystals suitable for X-ray diffraction analysis were grown by the vapor diffusion of diethyl ether into a concentrated solution of the product in dichloromethane.

Synthesis of Silver Complex 5c. Imidazolium salt **3c** (0.62 g, 1.53 mmol) and silver oxide (0.36 g, 1.53 mmol) were dissolved in dichloromethane (30 mL) and heated at reflux for 18 h in the dark. The mixture was filtered over Celite and the solvent removed from the filtrate *in vacuo* to give a colorless oil. Recrystallization from dichloromethane/diethyl ether gave the product as a white solid. Yield: 0.21 g (26%). ^{1}H NMR (300 MHz, $CDCl_3$): δ 7.37−7.18 (m, 15H, aromatic), 7.05 (s, 1H, NCH), 6.93 (s, 1H, NCH), 4.13 (t, 2H, CH_2), 1.80 (quin, 2H, CH_2), 1.31 (sext, 2H, CH_2), 0.93 (t, 2H, CH_2). ^{13}C{^{1}H} NMR (75 MHz, $CDCl_3$): δ 147.0 (C), 137.2 (CH), 129.7 (CH), 129.4 (CH), 129.1 (CH), 128.0 (CH), 127.8 (CH), 124.0 (CH), 122.6 (CH), 79.7 (C) 50.6 (CH_2), 32.4 (CH_2), 19.6 (CH_2), 13.6 (CH_3). HRMS (ESI+): calcd for $C_{52}H_{52}AgN_4$ [2M − $AgCl_2$]$^+$, 841.3240; found, 841.3245. Anal. Calcd for $C_{26}H_{26}AgClN_2$: C, 61.25; H, 5.14; N, 5.49. Found: C, 61.60; H, 5.15; N, 5.40. Single crystals suitable for X-ray diffraction analysis were grown by the vapor diffusion of diethyl ether into a concentrated solution of the product in methanol.

Synthesis of Silver Complex 5d. Imidazolium chloride **3d** (0.086 g, 0.19 mmol) and silver oxide (0.027 g, 0.12 mmol) were dissolved in a mixture of anhydrous methanol (5 mL) and dichloromethane (5 mL) in a Schlenk flask with activated 4 Å molecular sieves. The mixture was stirred at room temperature for 24 h in the dark. The mixture was filtered over Celite and the solvent removed from the filtrate *in vacuo* to give a light yellow solid. Yield: 0.01 g (10%). ^{1}H NMR (300 MHz, $CDCl_3$): δ 7.45−6.88 (m, 22H, aromatic and NCH), 4.54 (s, 2H, CH_2). ^{13}C{^{1}H} NMR (125 MHz, $CDCl_3$): δ 186.6 (C), 184.1 (C), 142.3 (C), 135.8 (C), 130.1 (CH), 129.9 (CH), 129.0 (CH), 128.5 (CH), 128.3 (CH), 127.4 (CH), 124.3 (CH), 119.6 (CH), 77.4 (C), 65.9 (CH_2). HRMS (ESI+): calcd for $C_{58}H_{48}AgN_4$ [2M − $AgCl_2$]$^+$, 909.2927; found, 909.2964. Anal. Calcd for $C_{232}H_{192}Ag_5Cl_5N_{16}$, i.e. 2:3 Ag(NHC)Cl:[Ag(NHC)$_2$]Cl: C, 71.07; H, 4.94; N, 5.72. Found: C, 70.80; H, 5.30; N, 5.60. Single crystals suitable for X-ray diffraction analysis were grown by the vapor diffusion of diethyl ether into a concentrated solution of the product in dichloromethane.

Synthesis of Silver Complex 5e. Imidazolium salt **3e** (0.1 g, 0.26 mmol) and silver oxide (0.04 g, 0.15 mmol) were dissolved in a solvent mixture of anhydrous methanol (10 mL) and anhydrous dichloromethane (5 mL) in a Schlenk flask. The mixture was stirred at room temperature for 24 h in the dark. The mixture was filtered over Celite and the solvent removed from the filtrate *in vacuo* to give a white solid. Yield: 0.018 g (14%). ^{1}H NMR (300 MHz, d_4-MeOD): δ 7.63 (broad s, 1H, NCH), 7.48−7.00 (m, 15H, aromatic), 6.86 (broad s, 1H, NCH), 4.12 (t, 2H, CH_2), 3.81(t, 2H, CH_2). ^{13}C{^{1}H} NMR (75 MHz, d_4-MeOD): δ 144.0 (C), 131.4 (CH), 129.4 (CH), 129.2 (CH), 124.5 (CH), 120.8 (CH), 78.6 (C), 62.4 (CH_2), 56.3 (CH_2). HRMS (ESI+): calcd for $C_{48}H_{44}AgN_4O_2$ [2M − $AgCl_2$]$^+$, 817.2512; found, 817.2529. Anal. Calcd for $C_{144}H_{132}Ag_5Cl_5N_{12}O_6$, i.e. 4:1 Ag(NHC)Cl:[Ag(NHC)$_2$]Cl: C, 60.83; H, 4.68; N, 5.91. Found: C, 60.80; H, 4.50; N, 5.80.

Synthesis of Silver Complex 6a. Imidazolium salt **1a** (0.40 g, 0.84 mmol) and silver oxide (0.19 g, 0.84 mmol) were dissolved in dichloromethane (40 mL) and heated at reflux for 24 h in the dark. The solution was filtered over Celite and the solid washed with dichloromethane. The solvent was removed from the filtrate *in vacuo* to give the product as a white crystalline solid. Yield: 0.21 g (43%). ^{1}H NMR (300 MHz, $CDCl_3$): δ 7.34−6.95 (m, 16H, aromatic), 3.88 (s, 3H, CH_3). ^{13}C{^{1}H} NMR (75 MHz, d_6-DMSO): δ 139.8 (C), 134.8 (C), 132.2 (C), 131.0 (CH), 130.2 (CH), 128.2 (CH), 128.1 (CH), 127.8 (CH), 123.2 (CH), 121.1 (CH), 118.5 (CH), 76.8 (CH), 40.1 (CH_3). HRMS (ESI+): calcd for $C_{46}H_{38}AgCl_2N_4$ [2M − AgI_2]$^+$, 825.1516; found, 825.1532. Anal. Calcd for $C_{23}H_{19}AgClIN_2{\cdot}3/2CH_2Cl_2$: C, 40.81; H, 3.08; N, 3.89. Found: C, 40.90; H, 3.20; N, 4.10.

Synthesis of Silver Complex 6c. Imidazolium salt **1c** (0.15 g, 0.28 mmol) and silver oxide (0.07 g, 0.28 mmol) were dissolved in dichloromethane (15 mL) and heated at reflux for 24 h in the dark. The solution was filtered over Celite and the solid washed with dichloromethane. The solvent was removed from the filtrate *in vacuo* to give a yellow solid, which was recrystallized from dichloromethane/pentane to give the product as a yellow solid. Yield: 0.08 g (47%). ^{1}H NMR (300 MHz, $CDCl_3$): δ 7.45−7.09 (m, 15H, aromatic and NCH), 6.96 (s, 1H, NCH), 4.15 (t, 2H, N−$CH_2CH_2CH_2CH_3$), 1.80 (dt, 2H, NCH$_2CH_2CH_2CH_3$), 1.32 (m, 2H, N−$CH_2CH_2CH_2CH_3$), 0.94 (dd, 3H, NCH$_2CH_2CH_2CH_3$). ^{13}C{^{1}H} NMR (75 MHz, $CDCl_3$): δ 141.1 (C), 140.0 (C), 135.8 (C), 131.6 (CH), 130.7 (CH), 130.6 (CH), 128.5 (CH), 128.2 (CH), 128.1 (CH), 123.6 (CH), 118.2 (CH), 77.8 (C), 53.6 (CH_2), 33.5 (CH_2) 19.7 (CH_2), 13.8 (CH_3). HRMS (ESI+): calcd for $C_{52}H_{50}AgCl_2N_4$ [2M − AgI_2]$^+$, 909.2460; found, 909.2609. Anal. Calcd for $C_{26}H_{25}AgClIN_2{\cdot}2/3C_5H_{12}$: C, 51.52; H, 4.86; N, 4.10. Found: C, 51.90; H, 5.20; N, 4.00. Single crystals suitable for X-ray diffraction analysis were grown by the vapor diffusion of pentane into a concentrated solution of the product in dichloromethane.

Synthesis of Silver Complex 6e. Imidazolium salt **1e** (0.32 g, 0.63 mmol) and silver oxide (0.14 g, 0.63 mmol) were dissolved in dichloromethane (30 mL) and heated at reflux for 24 h in the dark. The solution was filtered over Celite and the solid washed with dichloromethane. The solvent was removed from the filtrate *in vacuo* to give the product as a white solid. Yield: 0.12 g (31%). ^{1}H NMR (300 MHz, d_4-MeOD): δ 7.00−6.55 (m, 16H, aromatic and NCH), 3.83 (m, 2H, N−CH_2CH_2OH), 3.45 (m, 2H, N−CH_2CH_2OH). ^{13}C{^{1}H} NMR (75 MHz, $CDCl_3$): δ 140.9 (C), 140.2 (C), 135.8 (C), 132.5 (CH), 131.5 (CH), 130.7 (CH), 130.4 (CH), 128.4 (CH), 128.1 (CH), 127.8 (CH), 123.2 (CH) 120.1 (CH), 77.3 (C), 62.6 (CH_2), 55.6 (CH_2). HRMS (ESI+): calcd for $C_{48}H_{42}AgCl_2N_4O_2$ [2M − I]$^+$, 887.1883; found, 887.1864. Anal. Calcd for $C_{48}H_{42}AgCl_2IN_4O_2{\cdot}1/2CH_2Cl_2$: C, 55.22; H, 4.11; N, 5.31. Found: C, 55.20; H, 3.80; N, 5.00.

https://dx.doi.org/10.1021/acs.organomet.0c00069
Organometallics XXXX, XXX, XXX−XXX

Cytotoxicity Studies. Cells were incubated in 96-well plates, at 2 × 10^3 cells per well in 200 μL of growth media (RPMI 1640 supplemented with 10% fetal calf serum, sodium pyruvate (1 mM), and L-glutamine (2 mM). Cells were incubated for 24 h at 37 °C in an atmosphere of 5% CO_2 prior to drug exposure. Silver compounds and cisplatin were dissolved in dimethyl sulfoxide at a concentration of 25 mM and diluted with medium to obtain drug solutions ranging from 50 to 0.049 μM. The final dimethyl sulfoxide concentration was 0.1% (v/v), which is nontoxic to cells. Drug solutions were applied to cells and the cells incubated for 96 h at 37 °C under an atmosphere of 5% CO_2. The solutions were removed from the wells, and fresh medium was added to each well along with 20 μL of MTT (5 mg mL^{-1}), and the mixture incubated for 4 h at 37 °C under an atmosphere of 5% CO_2. The solutions were removed, and 150 μL of dimethyl sulfoxide was added to each well to dissolve the purple formazan crystals. A plate reader was used to measure the absorbance at 540 nm. Lanes containing medium only and cells in medium only (no drug) were used as blanks for the spectrophotometer and 100% cell survival, respectively. Cell survival was determined as the absorbance of treated cells divided by the absorbance of controls and expressed as a percentage. The concentration required to kill 50% of cells (IC_{50}) was determined from plots of percent survival against drug concentration. The results were expressed as the mean standard deviation for three independent experiments. All compounds and cisplatin were initially tested against Panc 10.05 (pancreatic cancer cell line) and ARPE-19 (noncancer retinal epithethial cell line). The selectivity index (SI) was determined (defined as the mean IC_{50} for ARPE-19 cells divided by the mean IC_{50} for Panc10.05 cells). Any compound with an SI value greater than cisplatin was selected for further evaluation against two other cancer cell lines (MiaPaCa-2 and BE). A selection of compounds with SI values lower than that of cisplatin was also tested in order to determine whether or not SI values against MiaPaCa-2 and BE cell lines remained low or whether cell-dependent variations were observed. Statistical analysis was conducted using a *t* test with significance defined as $p < 0.05$ or $p < 0.01$.

Hydrophobicity Measurements. Equal volumes of octanol and NaCl-saturated water were stirred at room temperature for 24 h and separated to give octanol-saturated water and water-saturated octanol. Accurate amounts of the complexes were dissolved in the water-saturated octanol (25 mL). A 3 mL portion of octanol-saturated water was placed in a centrifuge tube, and 3 mL of water-saturated octanol containing the complex was layered on top. The samples were shaken for 4 h using a Vibrax machine at 500g min^{-1}. The layers were separated, and the water-saturated octanol layer was retained for analysis using UV/vis spectroscopy. Using the maximum absorbance for each complex, the average of six runs was calculated, and rearrangement of individual calibration graphs gave the final $[C]_{org}$ value. The $[C]_{org}$ and $[C]_{aq}$ values were used to determine the partition coefficient log *P*.

Biomembrane Sensing Device. Full details of the device, the apparatus used, and operation are fully described in a previous publication.[56] A microfabricated Pt/Hg electrode coated with DOPC (Avanti Polar Lipids, Alabaster, AL, US, >99% purity) was contained in a sealed flow cell. In the RCV experiments the fabricated rectangular platinum electrode on the wafer was employed as a counter electrode and a Ag/AgCl/3.5 M KCl reference electrode was inserted into the flow cell. All potentials in this paper are quoted versus this reference electrode. A constant flow of 0.1 M KCl, calcined at 600 °C for 2 h and buffered at pH 7.4 with 0.01 M phosphate (hereinafter referred to as phosphate-buffered saline or PBS) was passed over the Pt/Hg electrode using a peristaltic pump. The electrodes were connected to a potentiostat (PGSTAT 30 Autolab potentiostat Ecochemie, Utrecht, The Netherlands) interfaced to a Powerlab signal generator (AD Instruments Ltd.) and controlled by Scope(c) software. Rapid cyclic voltammetry (RCV) scans were obtained by applying a sawtooth waveform from −0.4 to −1.2 V with a ramp rate of 40 V s^{-1} applied to the electrode surface. In the absence of Faradaic reactions, the current on the RCV plot is directly proportional to the capacitance of the surface and is displayed as a function of voltage. In response to the applied voltage ramp, the DOPC monolayers undergo two pronounced phase transitions characterized by two capacitance current peaks. These peaks correspond to structural changes of, and the redistribution of charges and polar groups on, the monolayer interface. All assays were carried out in pH 7.4 PBS with continuous scanning from −0.4 to −1.2 V. The compounds were tested for 400 s, after which PBS was flushed through for 400 s to allow for any recovery of the DOPC layer initial structure to take place. Both compound interaction and DOPC layer depuration took place with the monolayer undergoing two disruptive reversible phase transitions where each molecule of lipid is in contact with the aqueous phase. Increasing the concentration of the compounds in test media gave rise to increased responses following compound interaction with the DOPC layer. This was shown as enhanced peak suppression. The effect of compound dose on the RCV plot emphasizes the effect of compound type on the nature of and sensitivity to their interaction with the DOPC-coated electrode. The degree of RCV scan recovery is related to the degree of DOPC structure restoration, which in turn is related to the degree of reversibility of the interaction.

The LOD was measured by plotting a calibration graph of capacitance current peak height vs compound solution concentration following interaction with the respective compound. Subsequently the reproducibility of the capacitance current peak height from the RCVs of the DOPC-coated Hg electrode in PBS was estimated by taking 10 replicate measurements. The 3 times standard deviation (SD) of this capacitance peak height was calculated as a control. Accordingly the concentration of the test compound, which has an equivalent suppressive effect on the capacitance current peak height relating to 3 times the SD of the control, was read off the calibration curve to estimate the detection limit values. The detection limits were estimated and quoted as the minimum concentration of compound in water to elicit a response and these detection limits are related to compound molecular structure and the known biological effect of each compound. The LOD is inversely proportional to the ability of the compound to disrupt the layer structure and organization.

■ ASSOCIATED CONTENT

Supporting Information

The Supporting Information is available free of charge at https://pubs.acs.org/doi/10.1021/acs.organomet.0c00069.

X-ray crystallographic information, expanded RCVs, and NMR spectra (PDF)

Accession Codes

CCDC 1949011−1949023 contain the supplementary crystallographic data for this paper. These data can be obtained free of charge via www.ccdc.cam.ac.uk/data_request/cif, or by emailing data_request@ccdc.cam.ac.uk, or by contacting The Cambridge Crystallographic Data Centre, 12 Union Road, Cambridge CB2 1EZ, UK; fax: +44 1223 336033.

■ AUTHOR INFORMATION

Corresponding Authors

Roger M. Phillips − *School of Applied Sciences, University of Huddersfield, Huddersfield HD1 3DH, U.K.*; Email: R.M.Phillips@hud.ac.uk

Andrew Nelson − *School of Chemistry, University of Leeds, Leeds LS2 9JT, U.K.*; Email: A.L.Nelson@leeds.ac.uk

Charlotte E. Willans − *School of Chemistry, University of Leeds, Leeds LS2 9JT, U.K.*; orcid.org/0000-0003-0412-8821; Email: c.e.willans@leeds.ac.uk

Authors

Heba A. Mohamed − *School of Chemistry, University of Leeds, Leeds LS2 9JT, U.K.*

Samantha Shepherd − *School of Applied Sciences, University of Huddersfield, Huddersfield HD1 3DH, U.K.*

https://dx.doi.org/10.1021/acs.organomet.0c00069
Organometallics XXXX, XXX, XXX−XXX

Nicola William − *School of Chemistry, University of Leeds, Leeds LS2 9JT, U.K.*
Helen A. Blundell − *School of Chemistry, University of Leeds, Leeds LS2 9JT, U.K.*
Madhurima Das − *School of Chemistry, University of Leeds, Leeds LS2 9JT, U.K.*
Christopher M. Pask − *School of Chemistry, University of Leeds, Leeds LS2 9JT, U.K.*
Benjamin R. M. Lake − *School of Chemistry, University of Leeds, Leeds LS2 9JT, U.K.;* orcid.org/0000-0002-5775-1230

Complete contact information is available at: https://pubs.acs.org/10.1021/acs.organomet.0c00069

Author Contributions

All authors have given approval to the final version of the manuscript. The authors declare no competing financial interests.

Funding

The work was funded through the Universities of Leeds and Huddersfield, NERC (UK) grant NE/M021378/1, and the EU HORIZON 2020 HISENTS program grant agreement number 685817.

Notes

The authors declare no competing financial interest.

REFERENCES

(1) Rosenberg, B.; Van Camp, L.; Krigas, T. Inhibition of Cell Division in Escherichia coli by Electrolysis Products from a Platinum Electrode. *Nature* **1965**, *205* (4972), 698−699.
(2) Galanski, M.; Jakupec, M.; Keppler, B. Update of the Preclinical Situation of Anticancer Platinum Complexes: Novel Design Strategies and Innovative Analytical Approaches. *Curr. Med. Chem.* **2005**, *12* (18), 2075−2094.
(3) Brabec, V.; Kasparkova, J. Modifications of DNA by platinum complexes: Relation to resistance of tumors to platinum antitumor drugs. *Drug Resist. Updates* **2005**, *8* (3), 131−146.
(4) Almodares, Z.; Lucas, S. J.; Crossley, B. D.; Basri, A. M.; Pask, C. M.; Hebden, A. J.; Phillips, R. M.; McGowan, P. C. Rhodium, Iridium, and Ruthenium Half-Sandwich Picolinamide Complexes as Anticancer Agents. *Inorg. Chem.* **2014**, *53* (2), 727−736.
(5) Bergamo, A.; Sava, G. Ruthenium anticancer compounds: myths and realities of the emerging metal-based drugs. *Dalton Trans.* **2011**, *40* (31), 7817−7823.
(6) Rodriguez-Barzano, A.; Lord, R. M.; Basri, A. M.; Phillips, R. M.; Blacker, A. J.; McGowan, P. C. Synthesis and anticancer activity evaluation of [small eta]5-C5(CH3)4R ruthenium complexes bearing chelating diphosphine ligands. *Dalton Trans.* **2015**, *44* (7), 3265−3270.
(7) Wani, W. A.; Baig, U.; Shreaz, S.; Shiekh, R. A.; Iqbal, P. F.; Jameel, E.; Ahmad, A.; Mohd-Setapar, S. H.; Mushtaque, M.; Ting Hun, L. Recent advances in iron complexes as potential anticancer agents. *New J. Chem.* **2016**, *40* (2), 1063−1090.
(8) Lord, R. M.; Mannion, J. J.; Hebden, A. J.; Nako, A. E.; Crossley, B. D.; McMullon, M. W.; Janeway, F. D.; Phillips, R. M.; McGowan, P. C. Mechanistic and Cytotoxicity Studies of Group IV β-Diketonate Complexes. *ChemMedChem* **2014**, *9* (6), 1136−1139.
(9) Alessio, E.; Messori, L. 5. The Deceptively Similar Ruthenium-(III) Drug Candidates KP1019 and NAMI-A Have Different Actions. What Did We Learn in the Past 30 Years? *Metallo-Drugs: Development and Action of Anticancer Agents* **2018**, *18*, 141.
(10) Klasen, H. J. A historical review of the use of silver in the treatment of burns. II. Renewed interest for silver. *Burns* **2000**, *26* (2), 131−138.
(11) Banti, C. N.; Hadjikakou, S. K. Anti-proliferative and anti-tumor activity of silver(I) compounds. *Metallomics* **2013**, *5* (6), 569−596.
(12) Youngs, W. J.; Knapp, A. R.; Wagers, P. O.; Tessier, C. A. Nanoparticle encapsulated silver carbene complexes and their antimicrobial and anticancer properties: A perspective. *Dalton Trans.* **2012**, *41* (2), 327−336.
(13) Mohamed, H. A.; Willans, C. E. Silver-N-heterocyclic carbene complexes as promising anticancer compounds. *Organometallic Chemistry* **2014**, *39*, 26−50.
(14) Hopkinson, M. N.; Richter, C.; Schedler, M.; Glorius, F. An overview of N-heterocyclic carbenes. *Nature* **2014**, *510* (7506), 485−496.
(15) Praetorius, J. M.; Crudden, C. M. *N-Heterocyclic Carbenes: From Laboratory Curiosities to Efficient Synthetic Tools*; The Royal Society of Chemistry: 2011; p 77.
(16) Wang, M. H.; Scheidt, K. A. Cooperative Catalysis and Activation with N-Heterocyclic Carbenes. *Angew. Chem., Int. Ed.* **2016**, *55* (48), 14912−14922.
(17) Rajabi, F.; Thiel, W. R. An Efficient Palladium N-Heterocyclic Carbene Catalyst Allowing the Suzuki−Miyaura Cross-Coupling of Aryl Chlorides and Arylboronic Acids at Room Temperature in Aqueous Solution. *Adv. Synth. Catal.* **2014**, *356* (8), 1873−1877.
(18) Gil, W.; Trzeciak, A. M. N-Heterocyclic carbene-rhodium complexes as catalysts for hydroformylation and related reactions. *Coord. Chem. Rev.* **2011**, *255* (3−4), 473−483.
(19) Cavell, K. J.; Normand, A. T. In *N-Heterocyclic Carbenes in Transition Metal Catalysis and Organocatalysis*; Springer: 2011; p 299.
(20) Lavallo, V.; Grubbs, R. H. Carbenes As Catalysts for Transformations of Organometallic Iron Complexes. *Science* **2009**, *326* (5952), 559−562.
(21) Jones, W. D. Diverse Chemical Applications of N-Heterocyclic Carbenes. *J. Am. Chem. Soc.* **2009**, *131* (42), 15075−15077.
(22) Diez-Gonzalez, S.; Marion, N.; Nolan, S. P. N-Heterocyclic Carbenes in Late Transition Metal Catalysis. *Chem. Rev.* **2009**, *109* (8), 3612−3676.
(23) Glorius, F. *N-Heterocyclic carbenes in transition metal catalysis*; Springer-Verlag: Berlin Heidelberg, 2007.
(24) Roland, S.; Jolivalt, C.; Cresteil, T.; Eloy, L.; Bouhours, P.; Hequet, A.; Mansuy, V.; Vanucci, C.; Paris, J. M. Investigation of a Series of Silver-N-Heterocyclic Carbenes as Antibacterial Agents: Activity, Synergistic Effects, and Cytotoxicity. *Chem. - Eur. J.* **2011**, *17* (5), 1442−1446.
(25) Hindi, K. M.; Siciliano, T. J.; Durmus, S.; Panzner, M. J.; Medvetz, D. A.; Reddy, D. V.; Hogue, L. A.; Hovis, C. E.; Hilliard, J. K.; Mallet, R. J.; Tessier, C. A.; Cannon, C. L.; Youngs, W. J. Synthesis, stability, and antimicrobial studies of electronically tuned silver acetate N-heterocyclic carbenes. *J. Med. Chem.* **2008**, *51* (6), 1577−1583.
(26) Johnson, N. A.; Southerland, M. R.; Youngs, W. J. Recent Developments in the Medicinal Applications of Silver-NHC Complexes and Imidazolium Salts. *Molecules* **2017**, *22* (8), 1263.
(27) Panzner, M. J.; Hindi, K. M.; Wright, B. D.; Taylor, J. B.; Han, D. S.; Youngs, W. J.; Cannon, C. L. A theobromine derived silver N-heterocyclic carbene: synthesis, characterization, and antimicrobial efficacy studies on cystic fibrosis relevant pathogens. *Dalton Trans.* **2009**, *35*, 7308−7313.
(28) Hindi, K. M.; Panzner, M. J.; Tessier, C. A.; Cannon, C. L.; Youngs, W. J. The Medicinal Applications of Imidazolium Carbene-Metal Complexes. *Chem. Rev.* **2009**, *109* (8), 3859−3884.
(29) Kascatan-Nebioglu, A.; Panzner, M. J.; Tessier, C. A.; Cannon, C. L.; Youngs, W. J. N-Heterocyclic carbene-silver complexes: A new class of antibiotics. *Coord. Chem. Rev.* **2007**, *251* (5−6), 884−895.
(30) Kascatan-Nebioglu, A.; Melaiye, A.; Hindi, K.; Durmus, S.; Panzner, M. J.; Hogue, L. A.; Mallett, R. J.; Hovis, C. E.; Coughenour, M.; Crosby, S. D.; Milsted, A.; Ely, D. L.; Tessier, C. A.; Cannon, C. L.; Youngs, W. J. Synthesis from caffeine of a mixed N-heterocyclic carbene-silver acetate complex active against resistant respiratory pathogens. *J. Med. Chem.* **2006**, *49* (23), 6811−6818.

(31) Melaiye, A.; Simons, R. S.; Milsted, A.; Pingitore, F.; Wesdemiotis, C.; Tessier, C. A.; Youngs, W. J. Formation of water-soluble pincer silver(I)-carbene complexes: A novel antimicrobial agent. *J. Med. Chem.* **2004**, *47* (4), 973−977.
(32) Mohamed, H. A.; Lake, B. R. M.; Laing, T.; Phillips, R. M.; Willans, C. E. Synthesis and anticancer activity of silver(i)-N-heterocyclic carbene complexes derived from the natural xanthine products caffeine, theophylline and theobromine. *Dalton Trans.* **2015**, *44* (16), 7563−7569.
(33) Lv, G.; Guo, L.; Qiu, L.; Yang, H.; Wang, T.; Liu, H.; Lin, J. Lipophilicity-dependent ruthenium N-heterocyclic carbene complexes as potential anticancer agents. *Dalton Trans.* **2015**, *44* (16), 7324−7331.
(34) Bertrand, B.; Stefan, L.; Pirrotta, M.; Monchaud, D.; Bodio, E.; Richard, P.; Le Gendre, P.; Warmerdam, E.; de Jager, M. H.; Groothuis, G. M. M.; Picquet, M.; Casini, A. Caffeine-Based Gold(I) N-Heterocyclic Carbenes as Possible Anticancer Agents: Synthesis and Biological Properties. *Inorg. Chem.* **2014**, *53* (4), 2296−2303.
(35) Aher, S. B.; Muskawar, P. N.; Thenmozhi, K.; Bhagat, P. R. Recent developments of metal N-heterocyclic carbenes as anticancer agents. *Eur. J. Med. Chem.* **2014**, *81*, 408−419.
(36) Gautier, A.; Cisnetti, F. Advances in metal-carbene complexes as potent anti-cancer agents. *Metallomics* **2012**, *4* (1), 23−32.
(37) Wang, C. H.; Shih, W. C.; Chang, H. C.; Kuo, Y. Y.; Hung, W. C.; Ong, T. G.; Li, W. S. Preparation and Characterization of Amino-Linked Heterocyclic Carbene Palladium, Gold, and Silver Complexes and Their Use as Anticancer Agents That Act by Triggering Apoptotic Cell Death. *J. Med. Chem.* **2011**, *54* (14), 5245−5249.
(38) Teyssot, M. L.; Jarrousse, A. S.; Manin, M.; Chevry, A.; Roche, S.; Norre, F.; Beaudoin, C.; Morel, L.; Boyer, D.; Mahiou, R.; Gautier, A. Metal-NHC complexes: a survey of anti-cancer properties. *Dalton Trans.* **2009**, No. 35, 6894−6902.
(39) Hickey, J. L.; Ruhayel, R. A.; Barnard, P. J.; Baker, M. V.; Berners-Price, S. J.; Filipovska, A. Mitochondria-targeted chemotherapeutics: The rational design of gold(I) N-heterocyclic carbene complexes that are selectively toxic to cancer cells and target protein selenols in preference to thiols. *J. Am. Chem. Soc.* **2008**, *130* (38), 12570−12571.
(40) Siciliano, T. J.; Deblock, M. C.; Hindi, K. M.; Durmus, S.; Panzner, M. J.; Tessier, C. A.; Youngs, W. J. Synthesis and anticancer properties of gold(I) and silver(I) N-heterocyclic carbene complexes. *J. Organomet. Chem.* **2011**, *696* (5), 1066−1071.
(41) Medvetz, D. A.; Hindi, K. M.; Panzner, M. J.; Ditto, A. J.; Yun, Y. H.; Youngs, W. J. Anticancer Activity of Ag(I) N-Heterocyclic Carbene Complexes Derived from 4,5-Dichloro-1H-Imidazole. *Met.-Based Drugs* **2008**, *2008*, 1−7.
(42) Silver, S. Bacterial silver resistance: molecular biology and uses and misuses of silver compounds. *FEMS Microbiology Reviews* **2003**, *27* (2−3), 341−353.
(43) Sawyer, P. R.; Brogden, R. N.; Pinder, K. M.; Speight, T. M.; Avery, G. S. Clotrimazole: A Review of its Antifungal Activity and Therapeutic Efficacy. *Drugs* **1975**, *9* (6), 424−447.
(44) Sawyer, P. R.; Brogden, R. N.; Pinder, K. M.; Speight, T. M.; Avery, G. S. Clotrimazole: A Review of its Antifungal Activity and Therapeutic Efficacy. *Drugs* **1975**, *9* (6), 424−447.
(45) Benzaquen, L. R.; Brugnara, C.; Byers, H. R.; Gattoni-Celli, S.; Halperin, J. A. Clotrimazole inhibits cell proliferation in vitro and in vivo. *Nat. Med.* **1995**, *1* (6), 534−540.
(46) Gao, J.; Zhang, O.; Ren, J.; Wu, C.; Zhao, Y. Aromaticity/Bulkiness of Surface Ligands to Promote the Interaction of Anionic Amphiphilic Gold Nanoparticles with Lipid Bilayers. *Langmuir* **2016**, *32* (6), 1601−1610.
(47) Mohamadi, S.; Tate, D. J.; Vakurov, A.; Nelson, A. Electrochemical screening of biomembrane-active compounds in water. *Anal. Chim. Acta* **2014**, *813*, 83−89.
(48) Lake, B. R. M.; Willans, C. E. Structural Diversity of Copper(I)-N-Heterocyclic Carbene Complexes; Ligand Tuning Facilitates Isolation of the First Structurally Characterised Copper(I)-NHC Containing a Copper(I)-Alkene Interaction. *Chem. - Eur. J.* **2013**, *19* (49), 16780−16790.
(49) de Frémont, P.; Scott, N. M.; Stevens, E. D.; Ramnial, T.; Lightbody, O. C.; Macdonald, C. L. B.; Clyburne, J. A. C.; Abernethy, C. D.; Nolan, S. P. Synthesis of Well-Defined N-Heterocyclic Carbene Silver(I) Complexes. *Organometallics* **2005**, *24* (26), 6301−6309.
(50) Ramírez, J.; Corberán, R.; Sanaú, M.; Peris, E.; Fernandez, E. Unprecedented use of silver(i) N-heterocyclic carbene complexes for the catalytic preparation of 1,2-bis(boronate) esters. *Chem. Commun.* **2005**, No. 24, 3056−3058.
(51) Lin, I. J. B.; Vasam, C. S. Preparation and application of N-heterocyclic carbene complexes of Ag(I). *Coord. Chem. Rev.* **2007**, *251* (5−6), 642−670.
(52) Caytan, E.; Roland, S. Structure of Silver−N-Heterocyclic Carbenes in Solution: Evidence of Equilibration in DMSO at Very Different Time Scales by 1H NMR Experiments. *Organometallics* **2014**, *33* (8), 2115−2118.
(53) Rashid, A.; Vakurov, A.; Mohamadi, S.; Sanver, D.; Nelson, A. Substituents modulate biphenyl penetration into lipid membranes. *Biochim. Biophys. Acta, Biomembr.* **2017**, *1859* (5), 712−721.
(54) Furtado, C. M.; Marcondes, M. C.; Sola-Penna, M.; de Souza, M. L. S.; Zancan, P. Clotrimazole Preferentially Inhibits Human Breast Cancer Cell Proliferation, Viability and Glycolysis. *PLoS One* **2012**, *7* (2), e30462.
(55) Nelson, A. Electrochemical analysis of a phospholipid phase transition. *J. Electroanal. Chem.* **2007**, *601* (1), 83−93.
(56) Coldrick, Z.; Steenson, P.; Millner, P.; Davies, M.; Nelson, A. Phospholipid monolayer coated microfabricated electrodes to model the interaction of molecules with biomembranes. *Electrochim. Acta* **2009**, *54* (22), 4954−4962.
(57) Bizzotto, D.; Nelson, A. Continuing Electrochemical Studies of Phospholipid Monolayers of Dioleoyl Phosphatidylcholine at the Mercury−Electrolyte Interface. *Langmuir* **1998**, *14* (21), 6269−6273.
(58) Vakurov, A.; Galluzzi, M.; Podestà, A.; Gamper, N.; Nelson, A. L.; Connell, S. D. A. Direct Characterization of Fluid Lipid Assemblies on Mercury in Electric Fields. *ACS Nano* **2014**, *8* (4), 3242−3250.
(59) Ringstad, L.; Protopapa, E.; Lindholm-Sethson, B.; Schmidtchen, A.; Nelson, A.; Malmsten, M. An Electrochemical Study into the Interaction between Complement-Derived Peptides and DOPC Mono- and Bilayers. *Langmuir* **2008**, *24* (1), 208−216.
(60) Ormategui, N.; Zhang, S.; Loinaz, I.; Brydson, R.; Nelson, A.; Vakurov, A. Interaction of poly(N-isopropylacrylamide) (pNIPAM) based nanoparticles and their linear polymer precursor with phospholipid membrane models. *Bioelectrochemistry* **2012**, *87*, 211−219.
(61) Nelson, A.; Auffret, N.; Borlakoglu, J. Interaction of hydrophobic organic compounds with mercury adsorbed dioleoylphosphatidylcholine monolayers. *Biochim. Biophys. Acta, Biomembr.* **1990**, *1021* (2), 205−216.
(62) William, N.; Nelson, A.; Gutsell, S.; Hodges, G.; Rabone, J.; Teixeira, A. Hg-supported phospholipid monolayer as rapid screening device for low molecular weight narcotic compounds in water. *Anal. Chim. Acta* **2019**, *1069*, 98−107.
(63) Sanver, D.; Murray, B. S.; Sadeghpour, A.; Rappolt, M.; Nelson, A. L. Experimental Modeling of Flavonoid−Biomembrane Interactions. *Langmuir* **2016**, *32* (49), 13234−13243.
(64) Galluzzi, M.; Zhang, S.; Mohamadi, S.; Vakurov, A.; Podestà, A.; Nelson, A. Interaction of Imidazolium-Based Room-Temperature Ionic Liquids with DOPC Phospholipid Monolayers: Electrochemical Study. *Langmuir* **2013**, *29* (22), 6573−6581.
(65) Vakurov, A.; Brydson, R.; Nelson, A. Electrochemical Modeling of the Silica Nanoparticle−Biomembrane Interaction. *Langmuir* **2012**, *28* (2), 1246−1255.
(66) Protopapa, E.; Maude, S.; Aggeli, A.; Nelson, A. Interaction of Self-Assembling β-Sheet Peptides with Phospholipid Monolayers: The Role of Aggregation State, Polarity, Charge and Applied Field. *Langmuir* **2009**, *25* (5), 3289−3296.

https://dx.doi.org/10.1021/acs.organomet.0c00069
Organometallics XXXX, XXX, XXX−XXX

(67) Rashid, A.; Vakurov, A.; Nelson, A. Role of electrolyte in the occurrence of the voltage induced phase transitions in a dioleoyl phosphatidylcholine monolayer on Hg. *Electrochim. Acta* **2015**, *155*, 458−465.
(68) Holzer, A. K.; Manorek, G. H.; Howell, S. B. Contribution of the Major Copper Influx Transporter CTR1 to the Cellular Accumulation of Cisplatin, Carboplatin, and Oxaliplatin. *Mol. Pharmacol.* **2006**, *70* (4), 1390−1394.
(69) Sheldrick, G. A short history of SHELX. *Acta Crystallogr., Sect. A: Found. Crystallogr.* **2008**, *64* (1), 112−122.
(70) Sheldrick, G. Crystal structure refinement with SHELXL. *Acta Crystallogr., Sect. C: Struct. Chem.* **2015**, *71* (1), 3−8.

https://dx.doi.org/10.1021/acs.organomet.0c00069
Organometallics XXXX, XXX, XXX−XXX